Physics – Uspekhi **43** (7) 725 – 750 (2000)

FROM THE HISTORY OF PHYSICS PACS numbers: **01.65.+g**, 61.20.Qg, **73.20.–r**

Electrolysis and surface phenomena.

To the bicentenary of Volta's publication on the first direct-current source

A Ya Gokhshteĭn

DOI: 10.1070/PU2000v043n07ABEH000603

Contents

1. Introduction	**725**
2. Paradox di circolazione perpetua	**725**
3. Alternating surface tension of fluids and solids	**729**
4. Double cells at the phase boundary	**732**
5. Quantum insulation of discharge	**734**
6. Photoemission of secondary electrons	**736**
7. Spontaneous condensation of ionic atmosphere	**736**
8. Adsorption steps under exclusion of wave function nodes	**740**
9. Irreversible coating with memory	**745**
10. Membranes and their precursors	**746**
11. Conclusions	**749**
References	**749**

Abstract. The development of knowledge about electric current, potential, and the conversion of energy at the interface between electronic- and ionic-conductivity phases is briefly reviewed. Although soon after its discovery it was realized that electric current is the motion of charged particles, the double-layer field promoting charge transfer through the interface was considered for a long time to be as uniform as in a capacitor. One-dimensional ion discharge theory failed to explain the observed dependence of the current on the potential jump across the interface. The spatial segmentation of energy in the double layer due to the quantum evolution of the layer's periphery puts a limit on the charge transfer work the field may perform locally, and creates conditions for the ionic atmosphere being spontaneously compressed after the critical potential jump has been reached. A discrete interchange of states also occurs due to the adsorption of discharged particles and corresponds to the consecutive exclusion of the d-wave function nodes of metal surface atoms, the exclusion manifesting itself in the larger longitudinal and smaller lateral sizes of the atomic orbital. The elastic extension of the metal surface reduces the d-function overlap thus intensifying adsorption. Advances in experimentation, in particular new techniques capable of detecting alternating surface tension of solids, enabled these and some other phenomena to be observed.

A Ya Gokhshteĭn A N Frumkin Institute of Electrochemistry, Russian Academy of Sciences
Leninskiĭ prosp. 31, 117071 Moscow, Russian Federation
Tel. (7-095) 938-16 42, (7-095) 952-04 28. Fax (7-095) 952-08 46

Received 30 December 1999, revised 27 March 2000
Uspekhi Fizicheskikh Nauk **170** (7) 779 – 804 (2000)
Translated by Yu V Morozov; edited by A Radzig

1. Introduction

Alessandro Volta first reported on a new source of electric current in a letter to J Banks, the then President of the Royal Society of London, dated 20 March 1800. The letter written in French was read at a Royal Society meeting on June, 26 and soon published in the *Philosophical Transactions* (Vol. 90, 1800, pp. 403 – 431). The untitled original material was given a heading by Banks: "On the electricity excited by the mere contact of conducting substances of different kinds in a letter from Mr. Alexander Volta, F.R.S., Professor of Natural Philosophy at the University of Pavia..." [1].

The two hundred years that have since elapsed have been a time of the rapid progress in science and technology. Volta's discovery falls at the beginning of this period. It is difficult to find a physical phenomenon as universally applicable to the practical needs of man as this. Energy and information conversion, both in technology and nature, primarily depends on electric current, and there is still ample opportunity for further research in this field.

In the light of the impressive technological breakthrough of recent times scientific achievements do not look so amazing as they used to do in the past. However, new targets are as necessary as ever to ensure further progress. To overcome inertia of the known remains a major challenge to scientists working in line with historical traditions.

2. Paradox di circolazione perpetua

In everyday life, we usually think of electricity only when the power supply is cut off for some reason. But in the recent past, the mere possibility of a *continuous* circulation of electric fluid seemed almost improbable. Such thoughts were prompted by its peculiar salty taste which could be sensed when a circuit of two different metals was closed with the tongue. In his early

experiments, Volta worked with a short-circuited system and was unable to increase the current. It became a practical reality after a controllable device feeding the external circuit had been proposed.

In the first quarter of the 19th century, Volta's battery was the sole and widely used source of electric current. In 1807, H Davy succeeded in liberating metallic potassium and sodium from their liquid compounds by electrolysis (and was injured in an explosion). In August 1812, M Faraday came to work with him as a laboratory assistant.

The voltaic pile became a powerful tool for the observation of electrical phenomena which had previously been impossible to examine because of their pulsed nature. A simple experiment in which a conductor was heated by the passage of an electric current to verify the effect of heat on a magnetic needle brought H Oersted to the discovery of electromagnetism in the summer of 1820. An elastic suspension turned the needle into an instrument for measuring electric current. A Ampere's solenoid was the prototype of an elementary magnet. Faraday invented the first electric motor in 1821, discovered electromagnetic induction in 1831, and the laws of electrolysis in 1834. The latter discovery established the direct proportion between the amount of matter and the quantity of electricity carried by it. The progress would have been much slower had it not been for the invention of Volta's battery.

Thermoelectric effects were first observed by T Seebeck in 1821 and J Peltier in 1834. Both were based on the knowledge of electric current, acquired by their predecessors. H-armature electric generators were constructed by W Siemens in 1856. A lead-acid accumulator was proposed by G Planté in 1859.

Invention was not totally alien to J Maxwell. In 1858, he constructed the first color photographic camera. Also, he introduced his own concept of Saturn ring oscillations with a quantum-number type of wave orders and illustrated this theory with a mechanical model. The magnetic field around a capacitor being charged with an electric current was considered to be a manifestation of the wave process. In a letter to Faraday dated October 10, 1861, Maxwell reported about a new theory of electromagnetism. The complete version of Maxwell's theory was published in 1865, but it took 20 more years to draw attention despite its republishing in 1873 as a part of the two-volume encyclopedic edition under the title of *A Treatise on Electricity and Magnetism* [2].

As the President of the Physico-Mathematical Section, British Association for the Advancement of Science, Maxwell opened its 1870 annual meeting with a detailed review of recent progress in the field of physics. He mentioned as a noteworthy achievement (apparently with a subtle sense of humor) the hypothesis of W Thomson (later Lord Kelvin) concerning vortex motions in the incompressible ether. An opposite opinion assuming ether compressibility, Maxwell stated briefly without mentioning the author, presumably to spare the bewilderment of the audience, as follows: "Another theory of electricity which I prefer denies action at a distance and attributes electric action to tensions and pressures in an all-pervading medium, these stresses being the same in kind with those familiar to engineers, and the medium being identical with that in which light is supposed to be propagated" [3].

The words "...denies action at a distance" bring to mind the aforementioned time gap between the publication of the theory of electromagnetic waves and its universal acceptance. The distance which could not be overcome immediately required a giant step in the development of physical ideas. Analogies that could be found in the works of Volta and Maxwell served as a 'mechanical equivalent of truth' (similar to the mechanical equivalent of heat introduced by J Joule).

The source of electric current invented by Volta was a very simple construction, viz. a column consisting of a series of zinc and silver disks in pairs each of which was separated with a sheet of moist pasteboard. A column composed of tin and copper disks also produced electric current although twice weaker. Tin and copper are metals of the Bronze Age. They were used to make disk-shaped coins which were in circulation for thousands of years. Therefore, a pile responding to a touch by generating electric current might just as well have appeared 5000 years ago if it were a matter of technological development alone.

However, science offers no royal road to discovery which sometimes comes later than it might. It required a concurrence of circumstances to develop the idea of electricity, such as the elimination of the Inquisition, intensified communication between scholars, and free circulation of scientific information. Immediate impetus to the work in this field was given by L Galvani's treatise *De Viribus Electricitatis in Motu Musculari Commentarius* (Commentary on the Effect of Electricity on Muscular Motion) published in 1791 [4].

In Section 3, Galvani described, with many details and illustrations, muscular contraction in a frog extremity which he had examined when an exposed muscle was made an element of a *closed circuit* of two different conductors, either *two metals* or a *metal* and a *fluid* in which the muscle was embedded. Two pieces of the same metal failed to induce muscular action whereas a pair of iron and copper caused the muscle to contract. The contraction increased with the dissimilarity of metals, e.g. when a pair of iron and silver was used for the purpose. In other words, Galvani established *a certain sequence of metals* according to their ability to activate muscles when spanned by bimetallic arches. The substitution of insulators for conductors (oil for water or glass for metal) blocked muscular contraction. Galvani interpreted his findings as indicating *two outflows of the animal electricity* through a pair of different conductors. The problem was thus reduced to the search for a *site of decoupling between two opposite electricities* whose counter motion could account for the observed phenomenon — "...enim electricitatis excursus, atque circuitus demonstrantibus Physicis haberi, nisi in æquilibrii reparat one, atque vel solum, vel potissimum inter contrarias electricitates. In uno autem eodemque metallo latere illas omnino a natura alienum..." ("...because displacement of electricity, similar to the circular motion described by physicists, occurs — first and foremost — in no other way than at a restored equilibrium between two opposite charges. Their presence in the same metal is totally alien to nature...") [4].

Galvani believed that the decoupling of electricities occurred in the muscle and thus intuitively predicted the role of cell membranes. However, in his case, the membranes acted as amplifiers of an electric signal which was generated outside.

Galvani's work was published in the journal of the Bologna Academy of Sciences and as a booklet in 12 copies. The author presented one of the copies to Volta who had by that time been known for his works on electricity, invented an electrophorus (1775) and a flat capacitor (1780). An electric charge in Volta's electrophorus was produced by rubbing

against a *disk of a dielectric material* and induced on a *metallic disk*. The capacitor consisted of *two metallic disks* which could be *brought together*. The direction of further surveys was dictated by the *contact-over-area* principle.

Having begun his work in March, Volta reproduced Galvani's experiments and discussed the results in a few papers written in the first half of 1792. In November that year, the first report was published on the role of contacts in a closed circuit of dissimilar conductors, such as metals and an aqueous solution:

"È dunque fin qui tutto efetto di un tal combaciamento di metalli, nelle quali circonstanze non sona gia essi semplici *deferenti*, come in altre, me veri *motori* ad *eccitatori* di elettricita: e questa è una scoperta capitale." ("Therefore, the effect is entirely due to the said contact of metals which under the given conditions are not simply *conductors* (as in other cases) but also true *motors* and *exciters* of electricity: this is the main discovery.")

A sequence of metals listed in order of their mutual activity (zinc, tin, lead, iron, silver) was quoted by Volta in a letter of 20 May 1793 to T Cavallo who resided in England . He amended this list in another letter of 10 February 1794 addressed to A Vassali in Italy [1]. Volta emphasized the analogy between muscular contraction and gustatory sensation excited when the tongue was brought in contact with a pair of metals. It appears that Galvani's experiments provided the starting point for the consideration of the above sequence of metals. Later, Volta examined it based on his own observations of muscular contraction which turned out to be far more sensitive than the electrometers of those days.

Today, one can arrive at the same sequence of metals by measuring the potential difference between metal rods dipped into a weak saline solution (0.1 M NaCl). For example, the potential difference is 0.7 V for a (+)silver – lead(–) pair, and 0.4 V for a (+)silver – iron(–) pair. Taken together, these values represent a *series of electrode potentials in a solution* rather than the contact potential differences between metals (as some authors appear to erroneously believe). It reflects 'the work function required to withdraw an ion into the solution', not an electron into the vacuum.

Volta found that electric current was generated in a circuit containing *three* different conductors, either two metals and one solution or two solutions and one metal. In other words, he considered metals and solutions to be equally important electricity-producing media. This universal approach of Volta differed from the 'bimetallic contact theory of electric current', which spread spontaneously in the 19th century. Both Galvani and Volta deduced the crucial role of the metal – solution interface from experiments with a *single* metal. Volta described his variant of such an experiment in a letter of 1 August 1796 in the following way:

"Riempite una tazza di stagno con acqua di sappone, ...indi avendo impugnata codesta tazza con... ambedue le mani umettate d'acqua semplice, intigete l'apice della lingua nel liquore: vi farà sopresa l'inaspettata sensazione, che proverà la vostra lingua di un *sapore acido* al contatto del *liquore alcalino*. Un tal sapore... cagionata dalla corrente di fluido elettrico, che va dall'interiore della tazza di stagno al liquore contenuto, entra per la punta della lingua, ed attraversando questa e parte della persona, ritorna al medesimo metallo, ripassa nel liquore ecc. e mantiene par tal guisa una circolazione perpetua." ("Fill a tin bowl with soap water, take it in both hands moistened by natural water, and touch the liquid with the tip of your tongue. You will suddenly sense *acid taste* on the tongue despite its being in touch with the *alkaline liquid*. This sensation is caused by a flow of electric fluid which outgoes from the tin bowl into the soap water it contains, enters the tip of the tongue and, having passed through parts of the body, returns to the same metal and again traverses the water, thus maintaining a continuous circular motion.")

This experiment is easy to reproduce. Difficulties with the tongue do not arise. The tin bowl may be substituted by an aluminium one filled to capacity (2 litres) with water in which a table-spoonful of washing soda is dissolved. The electromotive force in the resulting circuit ('aluminium – soda solution – tongue and hand – water – aluminium') is 0.6 – 0.8 V, the same as in a circuit of two different metals. The electric current through the tongue is 20 – 50 μA.

In the same paper, Volta proposed a few variants of the electric circuit, one of which was formed by a series connection between two 'zinc – solution – silver' elements. One may be surprised at the three-year delay in the construction of the voltaic pile with 20 elements. It was caused by the fact that Volta was fairly well aware of the incompleteness of his explanation and tried to simplify the experimental conditions. Naturally, he had to first examine the boundary between the two conductors.

In another letter written in August 1796, Volta described a series of experiments designed to measure the polarity of metal plates following their disconnection. Zinc and silver were found to carry positive and negative charges, respectively. The letter of 23 March 1799 contained a description of a condenser electroscope which had been used to conduct these experiments (Fig. 1) [5]. A charge was repeatedly applied to the bottom plate covered with a layer of sealing-wax while the top one was earthed. Consecutive charges were accumulated in a capacitor. Pulling apart the two plates resulted in an enhanced deflection of silk filaments with elder balls suspended underneath. The disks served as the conductors to be examined. The charge was generated on the upper disk (zinc) by shortly letting it down to the bottom one (silver).

Bringing disks together is the critical but not the last step leading to a measurement of the contact potential difference. Widening the gap from a zero value is difficult to control, and calculations are complicated by the infinite initial charge problem. Later, the method of the dynamic condenser devised by Volta was modified and improved by F Kohlrausch, W Thomson, and W Zisman.

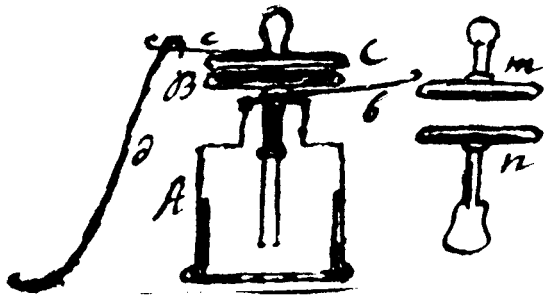

Figure 1. Experiment with a condenser electroscope and disks from dissimilar metals (a sketch by Volta): *A* — electrometer, *B* and *C* — bottom and top plates of the capacitor, *b* and *c* — plate terminals, *d* — conductor to earth the top plate, *m* and *n* — zinc and silver disks with handles.

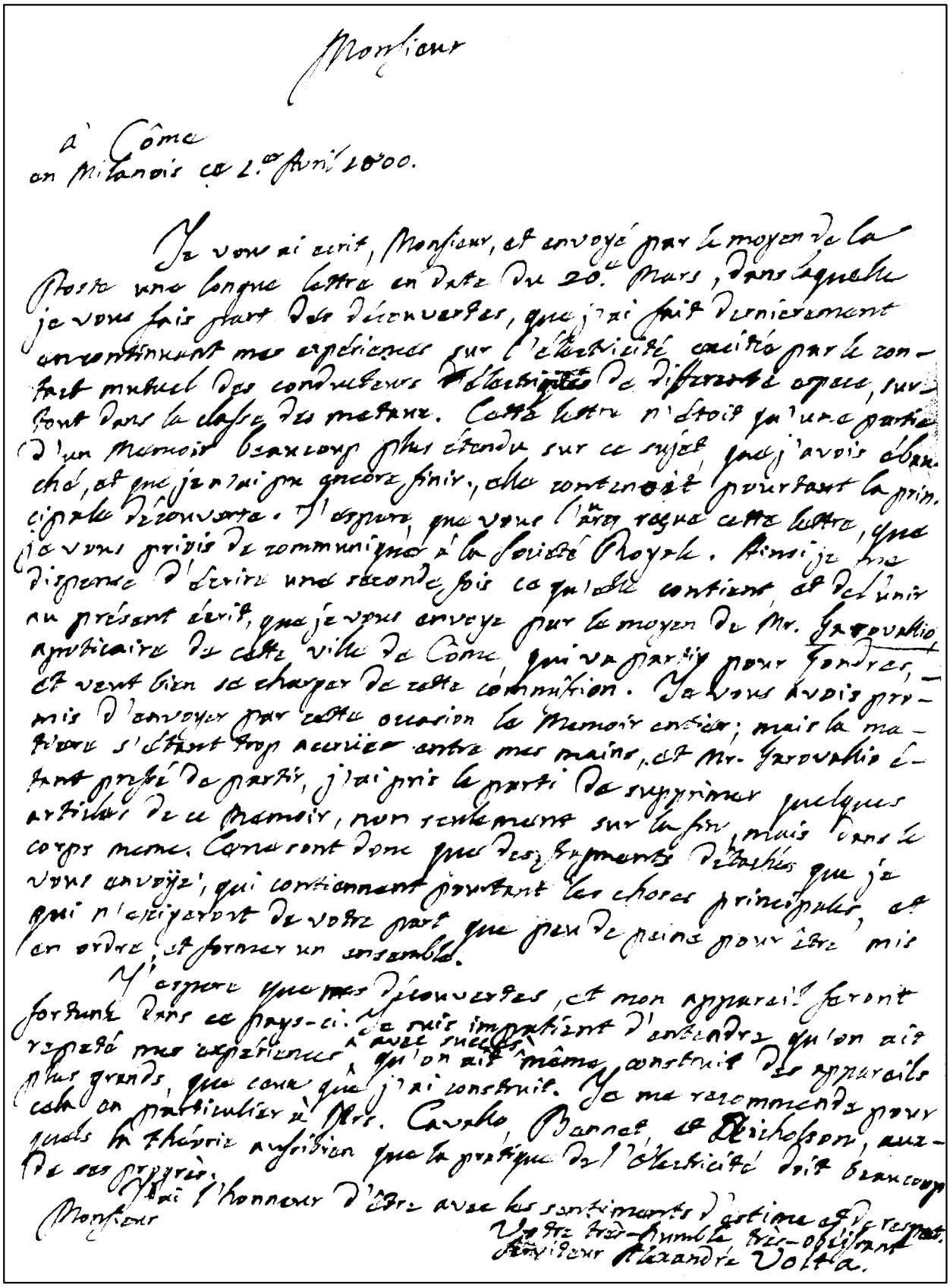

Monsieur

à Côme
en Milanois ce 1.er Avril 1800.

Je vous ai écrit, Monsieur, et envoyé par le moyen de la Poste une longue lettre en date du 20.e Mars, dans laquelle je vous fais part des découvertes, que j'ai fait dernièrement concernant mes expériences sur l'électricité excitée par le contact mutuel des conducteurs d'électricités de différente espèce, surtout dans la classe des métaux. Cette lettre n'étoit qu'une partie d'un Mémoir beaucoup plus étendu sur ce sujet que j'avois ébauché, et que je n'ai pu encore finir, elle contenoit pourtant la principale découverte. J'espère, que vous l'aurez reçue cette lettre, que je vous priois de communiquer à la Société Royale. Ainsi je me dispense d'écrire une seconde fois ce qu'elle contient, et de l'unir au présent écrit, que je vous envoye par le moyen de Mr. Zarovskio Apothicaire de cette ville de Côme, qui va partir pour Londres, et veut bien se charger de cette commission. Je vous avois promis d'envoyer par cette occasion le Mémoir entier; mais la matière s'étant trop accrûe entre mes mains, et Mr. Zarovskio étant pressé de partir, j'ai pris le parti de supprimer quelques articles de ce Mémoir, non seulement sur la fin, mais dans le corps même. Ce seront donc des fragments détachés que je vous envoye, qui contiennent pourtant les choses principales, et qui n'exigeront de votre part que peu de peine pour être mis en ordre, et former un ensemble.

J'espère que mes découvertes, et mon appareil feront fortune dans ce pays-ci. Je suis impatient d'entendre qu'on ait répété mes expériences, avec succès, qu'on ait même construit des appareils plus grands, que ceux que j'ai construit. Je me recommande pour cela en particulier à Mrs. Cavallo, Bennet, et Nicholson, auxquels la théorie indifférente que la pratique de l'électricité doit beaucoup de ses progrès.

J'ai l'honneur d'être avec les sentiments d'estime et de respect
Monsieur
Votre très-humble très-obéissant serviteur Alexandre Volta.

In December 1799, Volta connected an electroscope to a circuit of three conductors. Series connection of elements led to the amplification of the signal and revealed unique properties of the pile. Volta sent a detailed description of the pile construction to London in a letter of 20 March 1800. After a span of only 11 days, it was followed by a shorter letter in which he laid down plans for further work and proposed that T Cavallo, A Bennet, and W Nicholson, members of the Royal Society, reproduced his experiments on a bigger pile.

The value of this short letter was in that Volta's recommendations concerning the construction of a new pile were immediately accepted by the addressees. In the same year, W Nicholson and A Carlisle succeeded in decomposing water into hydrogen and oxygen by electrolysis. This was the first application of direct electric current doing work in an external circuit and suggested the electrical nature of particle bonding in matter. Davy continued these studies by determining the quantity of reaction products. Regular features common to all reactions were later noticed by Faraday, but the start of the study was made in the experiments of 1800.

Here is a facsimile of Volta's letter of April 1, 1800 and its translation:

"Monsieur,

from Como
near Milan, 1 April 1800

I wrote to you and sent by mail a long letter of March 20 in which I described in part the discoveries I had made in the course of further experiments on electricity excited upon the mutual contact of dissimilar electrical conductors including those of the class of metals. That letter was none other than a fragment of a bigger Memoir on the subject which I had designed but not yet completed. Nevertheless, it contains the essence of the discovery. I hope that you will receive the said letter and ask you to present it to a meeting of the Royal Society. This would spare me the trouble of enclosing another description with the present letter which will be delivered to you by Mr Garovallio, apothecary of the town of Como. He is going to London and kindly consents to take up this commission. I promised you to use this opportunity and send you the full text of the Memoir, but the material in my hand accrues progressively, and Mr Garovallio can wait no longer. Therefore, I decided to abridge a few articles not only at the end of this Memoir, but in its central part as well. This curtailment does not apply to those isolated fragments which I sent you earlier; they contain all the major principles, and you will find no difficulty in putting them in order and bringing them together.

I do hope that my discoveries and my apparatus will promote further progress in this field. Also, I am impatient to hear that my experiments are successfully reproduced and bigger apparatuses than mine constructed. In this respect, I first and foremost rely on Messrs. Cavallo, Bennet, and Nicholson who have greatly contributed to the progress in the theory and practice of electricity.

I have the honour to express, Monsieur, my feelings of appreciation and respect.

Your most humble and obedient servant
Alessandro Volta"

In 1801, Volta was invited to visit France. He left Como on the 1st of September and, after a stay in Switzerland, arrived in Paris on 26 September to take part in the work of a scientific commission on galvanism. On November 7, 12 and 22, Volta delivered lectures at the French Institute where he demonstrated the experiments and read three parts of his Memoirs advocating the identity of electric and galvanic fluids. Volta's lectures were attended by Napoleon.

In Germany, two young men, A Humboldt and J Ritter, took special interest in the new phenomenon. Humboldt visited Volta in Como in 1795 and 1805. He repeated Volta's experiments and showed them to Ritter. In 1799, Ritter succeeded in reproducing electrolysis and noticed traces of chemical changes in metals immersed in a solution. In 1803, he constructed a storage battery which is referred to as Ritter's secondary pile in the *Treatise* by Maxwell. The results of Ritter's studies were published between 1800 and 1805. Poverty and illness prevented him from continuing the work.

One of the most powerful batteries was created by V V Petrov in Russia in 1802. Petrov managed to obtain an electric arc. A few years later, Davy's work in the same field led him to construct a light-providing device (1811). Davy visited Volta in Como in 1813. Faraday was present during their meeting (he accompanied the Davys on their European wedding tour which also pursued a scientific scheme).

The stock of data concerning the new phenomenon enlarged so rapidly that Volta decided to discontinue his studies along this line. The reason for which he did not use, in full measure, the powerful experimental tool created by himself remains unclear. He had enough time to make additional experiments, e.g. at least two months after he had dispatched his letters to London. It may be conjectured that Volta had many times observed intensive decomposition of water but delayed its in-depth examination and therefore chose to forbear comments on the subject. It can be inferred from his second letter that the amazing success of research induced Volta to largely concentrate on a detailed description of the new source of electric current, the improvement of its construction, and the development of the theory of the underlying phenomenon.

The origin of electric current in the battery was for a long time a matter of controversy. M Faraday, in his works published between 1834 and 1840, opposed the contact theory of electric current and indicated that, in the absence of an external source of heat, the *permanent* contact of two metals could not produce a long-lasting effect leading to the breakdown of other substances [6]. He demonstrated that the electromotive force resulted from the conversion of chemical energy into electrical energy at the interface between a metal and a solution. It followed from his findings that the electric current in a battery circuit could not flowed infinitely long. According to Faraday, the limited source of metal was to be finally exhausted, at variance with propositions of the contact theory.

3. Alternating surface tension of fluids and solids

The emergence of potential difference between the battery terminals is a well-known phenomenon. Can it be resolved into individual potential jumps inside the battery and how could they be measured, if at all? In 1853, H Helmholtz identified the boundary area with a flat-plate capacitor and introduced the notion of an electrical double layer containing oppositely charged particles of both the solution and metal [7]. The high capacitance of the electrolytic capacitors is employed in electronics. In the last decade, it has been used to create two-layer accumulators comparable with secondary sources of electric current in terms of size.

Notwithstanding the phenomenological similarity with a macroscopic capacitor, the double layer at the boundary between a metal and an electrolyte is an object of atomic width, which provides a unique opportunity to study elementary processes. Observations of the shape of a mercury drop led to the discovery of electrocapillarity, i.e. the effect of the charge of a double layer on the surface tension of a liquid metal. In 1875, G Lippmann derived the

equation

$$\frac{\partial\gamma}{\partial E} = -q\,, \tag{3.1}$$

where γ is the surface tension, E is the electrode potential relative to that of the reference electrode, anf q is the surface density of the electrode charge, which governed the liquid medium at a constant temperature [8]. At a zero charge, the surface tension approaches its maximum, while the capacitance of the double layer is close to a minimum and continues to decrease as the solution is diluted.

Examining the same effect in 1903, B Kučera estimated mercury surface tension based on the drop weight and dropping period on falling from the capillary. In 1922, J Heyrovsky [9] continued these experiments as recommended by Kučera and showed that the addition of metal ions into the solution induced an electric current in a circuit of a dropping mercury electrode at the electric potentials corresponding to the place of each metal in a sequence of voltages. This observation has led to the development of a new analytical method, polarography.

The continuous growth of the dropping electrode complicated the construction of current – voltage curves. Today, a special device to automatically reproduce fixed drop electrodes [10] is widely used. A rod which closes the entrance to a mercury-filled capillary tube is raised with the aid of an electromagnet for a short controllable time (0.1 s). Specifically, this instrument ensures the stepwise enlargement of the electrode surface and allows a charge of the double layer to be measured from the current pulse.

It might be supposed that the potential jump across the boundary between a metal and a solution vanishes in the absence of the double layer (at its zero charge). However, experiments conducted by G Gouy in 1906 – 1908 yielded a different result [11]. Measurements of the surface tension of pure mercury and amalgam in the same solution demonstrated the existence of potential difference between two uncharged metals present in the solution. In 1928, A Frumkin showed that this phenomenon was identical to the contact potential difference between two metals in a vacuum [12, 13]. In this case there were no potential jumps at the boundaries between either metal and the solution. Frumkin developed a concept according to which the kinetics of surface processes are a function of the position of a zero-charge point. He provided numerous experimental data in support of this concept.

The state of the double layer also affects the surface tension of a solid [14]. However, this action conforms to a different law than that for a fluid, namely

$$\frac{\partial\gamma}{\partial E} = -q - \frac{\partial q}{\partial\Omega}\,, \tag{3.2}$$

where Ω is the relative elastic deformation of the surface, and $\gamma = \gamma(E, \Omega)$. In the general case, Eqn (3.2) is valid for an anisotropic solid (monocrystal), and γ and Ω are the surface tension and deformation tensors, respectively, while the term q is multiplied by a unit tensor. The simple scalar equation (3.2) is applicable in a sufficiently symmetric case, for instance, at the (100) surface of a metal with the face-centered cubic lattice, and also to polycrystalline objects.

Equation (3.2) gives rise to the expression for the slope of the $\partial\gamma/\partial q - E$ curve:

$$\frac{\partial}{\partial E}\left(\frac{\partial\gamma}{\partial q}\right) = -1 - \frac{1}{C}\,\frac{\partial C}{\partial\Omega} + C^2\,\frac{\partial\gamma}{\partial q}\,\frac{\partial^2 E}{\partial q^2}\,, \tag{3.3}$$

which contains only one unknown quantity $(\partial C/\partial\Omega)/C$, where $C = C_{\mathrm{d}} = \partial q/\partial E$ is the electrode differential capacitance.

The alternating surface tension is detected using a piezoelement (Fig. 2). Recording manipulations at the solid electrode surface are facilitated by that the lower side of an L-shape metal plate is in contact with the solution while its upper side is coupled to the piezoelement [14]. An electric

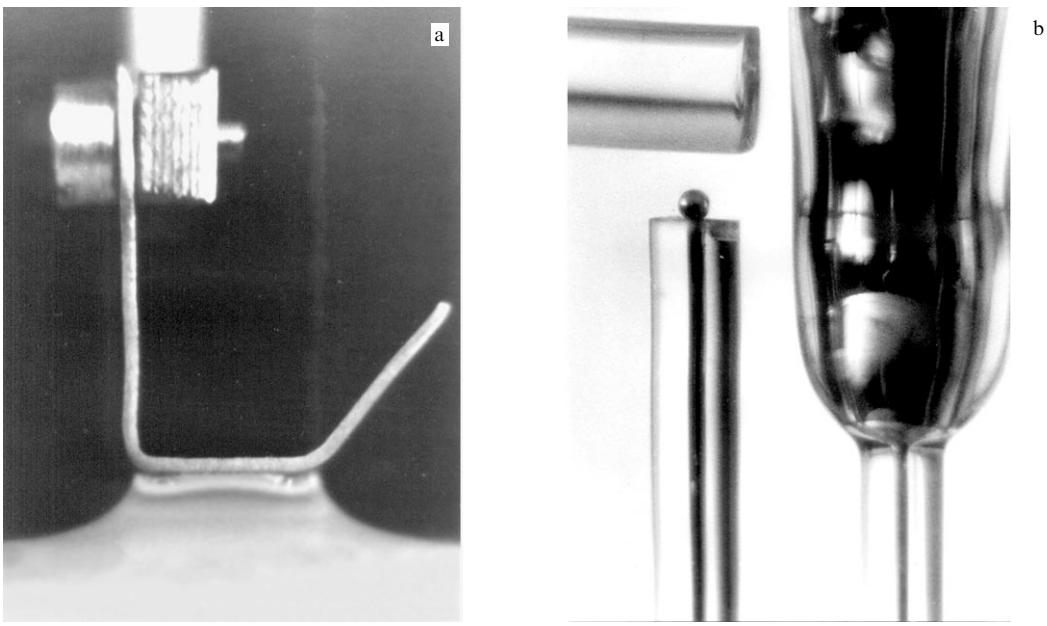

Figure 2. Methods used to detect surface tension oscillations of solid and liquid electrodes in the form of a plate (a) and a drop at the end of an U-shaped capillary tube (b). The plate holder and the rod coming to the drop from above are attached to a piezoelement. The wetted part of the plate is 5 mm long, and the capillary outer diameter is 3.2 mm.

current of frequency from 0.1 to 300 kHz causes the plate to vibrate with an amplitude of the order of 10^{-11} cm. The vibrations are resonantly perceived by the piezoelement. Alternate heating of the metal surface, e.g. by a light beam of the same frequency from a laser diode, serves as a reference. The light pressure proves to be relatively small. The diode is under direct voltage control up to a frequency of 1 MHz. The beam's distant action provides an additional opportunity for detecting surface tension, for instance, at high temperatures.

The derivative $\partial\gamma/\partial q = (\partial\gamma/\partial E)/(\partial q/\partial E)$, where $\partial q/\partial E > 0$, is measured in the experiment. The quantity $\partial\gamma/\partial q$ called *estance* has the dimension of the potential as a quotient obtained when energy (γ) is divided by charge (q) per unit surface. For this reason, the slope of the curve in coordinates $\partial\gamma/\partial q - E$ is a dimensionless quantity, which sometimes permits an easier physical interpretation of the results.

This technique is thus employed for detecting the alternating surface tension of the solids although this opportunity did not exist before. In terms of simplicity, sensitivity, reproducibility, and the spectrum of experimental conditions (e.g., frequency), this method of surface analysis is as efficient as that using an alternating current for determining the double layer capacitance (see several examples below). Moreover, it yields firsthand information which cannot be obtained by other methods. One of the simple advantages of the estance technique lies in that the signal comes directly from the surface, regardless of the frequency. In contrast, the impedance known since the 19th century and recorded with the aid of alternating current always includes the contribution of resistance in the solution volume, which tends to suppress the contribution of the double layer capacitance at frequencies of the order of tens of kilohertz.

In the simplest systems, the first term of Eqn (3.2) predominates; it reflects the electrostatic properties of the double layer. In this case, the dependences $\partial\gamma/\partial q - E$ and $\partial\gamma/\partial\varphi - E$ pass through the zero point near the zero-charge potential (Fig. 3). Anion adsorption increases the work function and, accordingly, shifts the zero-charge point towards negative values. This effect enhances in a series of SO_4^{2-}, Cl^-, Br^-, I^-, in that order. The second term of Eqn (3.2) is related to quantum phenomena, specifically to electron density redistribution at the interface. In the case of hydrogen adsorption, the second term is greater than the first; this difference is reflected in the multiplicity of zeroes attendant to $\partial\gamma/\partial q$ (see Section 8).

Elastic extension of a metal along the surface reduces the overlap between its atomic levels and therefore strengthens the adherence of the adsorbed atoms to the surface, which affects the $\partial q/\partial\Omega$ magnitude. The narrow d-zones of transition metals show especially strong dependence on the interatomic distance. An extension of platinum under conditions of a constant potential jump at the boundary between the metal and the solution leads to a rise in the number of adsorbed hydrogen atoms per unit area. As the filling increases, the affinity in the case of elastic extension amounts to $\partial G/\partial\Omega = -30\,\text{kcal mol}^{-1}$, where G is the energy expenditure on hydrogen adsorption.

When working with hard metals, one must take into account that they have a rough surface. Rolling and annealing plates of metals with a cubic structure enables one to fabricate uniform surfaces with a roughness factor close to 1. A smooth metallic surface may also be obtained by electropolishing. In other cases, the flat resultant of surface tension can be found by computation or by comparison of the

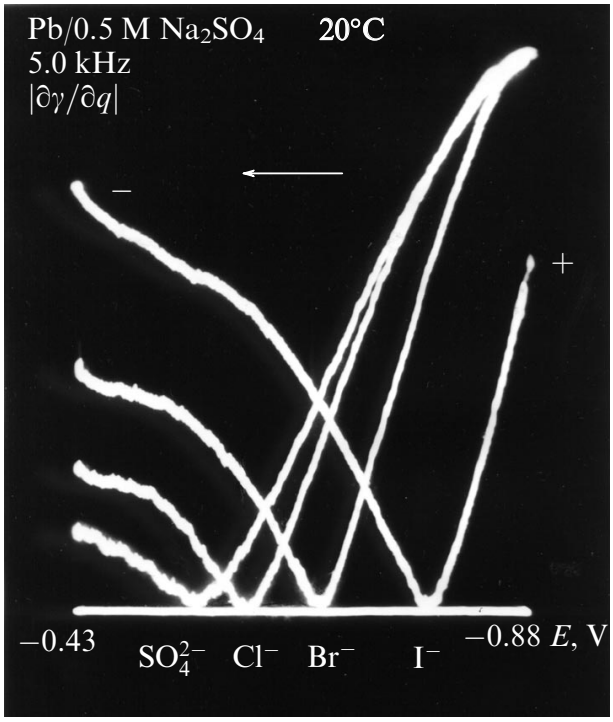

Figure 3. Shift of the zero-charge point in lead with increasing capacity of anions for adsorption. NaCl, NaBr, and NaI (0.15 M each) were consecutively added to the 0.5 M Na_2SO_4 solution. Lead electrode potential E is presented in the scale of the normal hydrogen electrode (NHE); temperature 20°C.

data obtained with specimens differing in roughness factors which are determined from the amount of the adsorbed substance. The ratio of the rough plate surface tension to the flat resultant coincides with the increment ratio of the corresponding areas in the case of uniform elastic extension of the plate.

Results of thermal modelling of surface tension indicate that the estance technique is also sensitive to heat release associated with adsorption. This effect is the surface analogue of the Peltier effect. The fundamental difference between the two consists however in that adsorption constitutes a change in the phase boundary composition absent in the natural Peltier effect when the electric current crosses the *unaltered* boundary between two different metals.

Thermal surface tension $\Delta\gamma_\tau$ induced by heat addition ΔW_τ to a sufficiently thin surface layer of a metal (before it spreads deeper) is of the same order of magnitude as the heat itself:

$$\Delta\gamma_\tau = -\frac{\varkappa_s Y_s}{\zeta_s \rho_s (1-\nu)}\,\Delta W_\tau\,, \tag{3.4}$$

where $\varkappa_s$ is the coefficient of linear thermal extension, Y_s is the modulus of elasticity, ζ_s is the specific heat capacity, ρ_s is the density, and ν is the Poisson coefficient of the metal under consideration. In platinum with a surface orientation (100), $\Delta\gamma_\tau \approx -\Delta W_\tau$ at 20 °C.

Heat release has been documented by the estance technique during anion adsorption on transition metals and in the case of charging the double layer at an oxidized surface, for example, that of platinum, where $\partial W_\tau/\partial q \approx -0.5$ V. The contribution of the heat liberated during hydrogen adsorp-

tion and in many other cases to the measured signal is negligibly small compared with that of surface tension. In any case, the two effects can be distinguished thanks to the phase difference resulting from the heat penetration deep into the metal and depending on the thickness of the metal plate. The possibility of excluding (if necessary) the contribution of surface tension is illustrated by Fig. 3. The contribution is absent at a point on the potential axis where the estance is zero. Also, such a situation can be created artificially by compensating for the contribution of surface tension with an external alternating force which arises in a constant magnetic field.

Ordinary electrocapillary curves at the boundary between a liquid metal and a solution can be obtained in the oscillation regime detected by the piezoelement. Differential recording and scanning of the potential enhance their informative value and accuracy (Fig. 4).

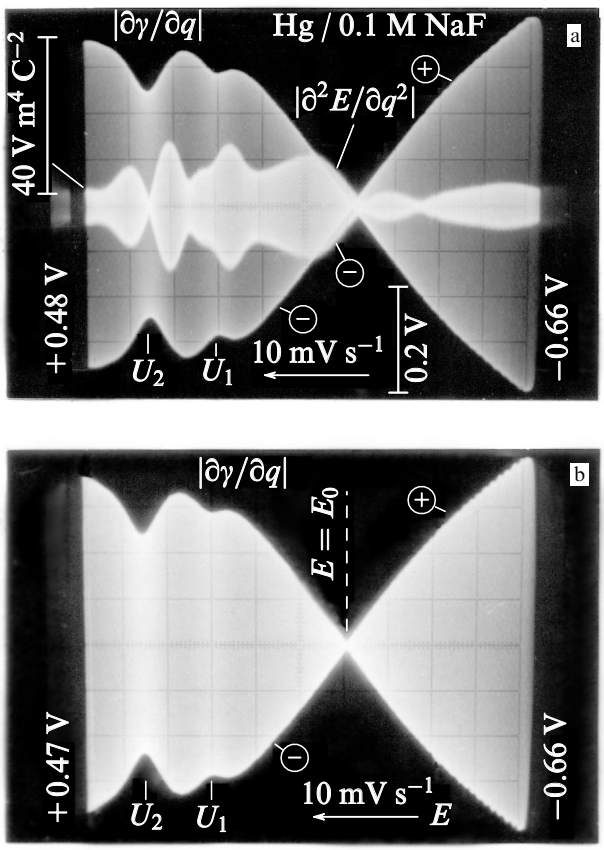

Figure 4. Differential electrocapillary curves for mercury in a 0.1 M NaF solution: (a) simultaneous recording of $|\partial\gamma/\partial q|$ and $|\partial^2 E/\partial q^2|$, (b) reproduced $|\partial\gamma/\partial q|$. U_1 and U_2 are the waves corresponding to the two stages of fluorine adsorption on mercury before a monolayer is formed. The diagram shows signs of derivatives $\partial\gamma/\partial q$ and $\partial^2 E/\partial q^2$ counted from the zero line (horizontal symmetry axis); scanning limits of E are given on the NHE scale; temperature 20°C.

4. Double cells at the phase boundary

The electromotive force in a cell of Volta's zinc – sulfuric acid solution – silver battery reached 1 V (in modern units). Closing the circuit resulted in zinc dissolution with the formation of Zn^{2+} ions and a concomitant discharge of hydrated hydrogen ions on the silver accompanied by gas release. Also, zinc dissolution leads to the liberation of energy. Part of this energy is utilized to discharge hydrogen ions and surmount the resistance of the solution. The rest is consumed in the external circuit.

Hydrogen release is a characteristic feature of voltaic cells containing metals in various combinations. Their construction was modified in 1836 when J Daniell proposed placing zinc and copper electrodes in the dissolved salts of these metals separated by a partition:

$$Zn \to Zn^{2+} + 2e^- \ (-)\,, \qquad Cu^{2+} + 2e^- \to Cu \ (+)\,.$$

With the circuit open, the metal and its ions are in equilibrium. The effect of the ion concentration on the equilibrium potential was first proved by W Nernst. If a single metal is used (as in the bowl experiment), the concentrations and even compositions of the two solutions must be different. It is impossible to resolve the electromotive force into individual measurable jumps. In contrast, a potential jump in an ionic double layer can be measured. A change of such a jump is responsible for overvoltage, i.e. the deviation from an equilibrium potential necessary to increase current density.

Energy conservation problem. The overvoltage is especially high when hydrogen is released on silver, copper, and mercury. In 1900 – 1905, J Tafel studied hydrogen release during electrolysis of aqueous solutions and obtained a logarithmic dependence of current density j on overvoltage η having a constant slope [15]. This relationship is governed by the equation

$$j = j_0 \exp \frac{\alpha e \eta}{kT}\,, \tag{4.1}$$

where j_0 is the exchange current density at equilibrium, T the temperature, k the Boltzmann constant, e the elementary charge, and $\alpha \approx 1/2$ the coefficient obtained experimentally; here, by definition, $\eta > 0$. In coordinates $\lg j - \eta$, the results have the form of straight lines in the η interval exceeding 1 V. This phenomenon has been described in many monographs (see, for instance, Refs [16 – 19].

The reaction rate normally shows an exponential dependence on energy expenditure. The amount of energy expended by an external source of electric current on an elementary event of discharge can be measured and is $W_s = e\eta$. In the experimental dependence (4.1), under the exponent is only *half* of this quantity, $e\eta/2$. An explanation is still being sought even now, the 100 years later.

Breakdown of flat equipotentiality. Difficulties inherent in the classical theory of discharge in the double layer are due to its axiomatic nature. Ion discharge by an electron was considered to occur in a stable field across an entire double layer functioning as a boundless flat capacitor. It was assumed that the electron overcomes a *constant* potential difference η, thus acquiring energy $W_s = e\eta$. In this line of reasoning, one weak point of the contact theory of current is fully preserved even if in a different form. *A source cannot release energy and remain unaltered.* The double layer which influences the discharge must in turn experience its reciprocal action. A double-layer vacancy that arises at the discharge site shows a local fall of the potential difference (practically to zero), in conflict with the axiom of the constancy of this quantity. The vacancy diameter corresponds to the mean distance between the *excess* ions which form the charge of the ionic atmosphere. The charging of the vacancy as a capacitor

is accompanied by a significant dissipation of energy which was not taken into account by early authors. The energy stored after the losses constitutes 'Tafel's half'.

The major source of energy during a discharge is not so much the entire double layer as its autonomous element, a double cell which conserves the energy stored (Fig. 5) [20–22]. The cell contains a minimum number of excessive opposite charges (in the simplest case — two) and exhibits the properties of a microcapacitor. Under conditions of thermal ion motion, cells differ in size but are characterized by a similar change of the potential and remain energetically independent.

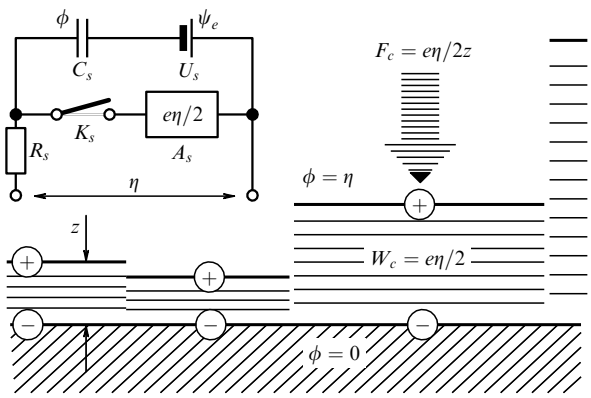

Figure 5. Autonomous cells of the double ionic layer at a common change η of the potential ϕ counted from the metallic electrode in the case of univalent ions: W_c — energy stored in the cell, F_c — force of attraction between an ion and the electrode, z — distance between the electrode and the center of the ion. Top left: an equivalent cell diagram for the weak peripheral field effect: C_s is the capacitor with charge e and capacitance e/η, U_s is the source of electromotive force ψ_e (difference between electrode equilibrium potential and zero-charge potential; in the main figure, $\psi_e = 0$), A_s is the energy consumer (electron transfer), K_s is the key, R_s is the medium resistance separating the given cell from all others. When the key closes the circuit, R_s- and ψ_e-independent energy $e\eta/2$ is fed to A_s.

An ion discharge is a limiting step which determines the electric current in the course of hydrogen release on silver (as in a voltaic cell), mercury, and similar sufficiently inert metals. Which charge (proton or electron) crosses the double layer during a discharge is a matter of conjecture. The present considerations apply to either case. The data presented below suggest an electron transfer which allows the discharge stage to be written in the form $H_3O^+ + e^- \to H_3O$ with a subsequent hydrogen adsorption and recombination, in particular, $H_3O \to H_{ad} + H_2O$, $2H_{ad} \to H_2$. The double cell $\{H_3O^+, e^-\}$ is formed by charging a free section of the interface. Such a section arises as a double vacancy following the previous discharge, i.e. a local charge deficit in the ionic atmosphere and electron cloud of the metal surface. The vacancy is charged by currents outgoing from the periphery of the double layer; the process takes approximately 10^{-10} s which is much longer than the time of electron transfer on ion discharge (10^{-15} s).

Because the distance between ions in the double layer is relatively large, the local potential is determined by the presence of an ion (as the plate of an equivalent microcapacitor). The micropotential follows the ion as it diffuses and falls on its discharge (and vanishes in the limiting case) whereas the neighboring ions preserve their micropotentials. Therefore, there is no unified potential distribution at the metal–solution interface, common to all the ions, as a function of the distance from the boundary (and as a solution of the one-dimensional Poisson equation). A macroscopic analogue is the undulating equipotential surface of a solution separated from the metal by an uneven insulating film. The motion of a charge in an ionic double layer is a multiparticle problem. Its limiting case is a totally isolated double cell.

Self-energy. One cell *completely expels* fields of the neighboring cells from its region. The only energy carrier in the region of an individual cell is the field created by its own charges. This may seem to be the result of superposition of the fields of all charges in the double layer. However, the effect of peripheral charges spreads with a delay, not only relativistic but, mainly, quantum. Therefore, the intrinsic energy of a cell W_c (*at a discharge*) is *really utilized* during rather a short time to ensure electron transfer, *without the involvement of other charges* (which are sufficiently remote at small η) or *with their limited participation*.

Upon the discharge of a univalent ion, an electron in the double-layer field acquires an energy $W_a = \alpha(e\eta) < e\eta$ with

$$\alpha = \vartheta + \chi\,, \tag{4.2}$$

where ϑ is the independence factor (the contribution of the cell's self-energy), and χ is the overlapping factor (the contribution of the energy of the remaining part of the double layer) growing with η; $\chi = 0$ for $\eta = 0$, $\chi \ll \vartheta$. The natural separation of energy into two constituents (internal and external) forms the conceptual basis for the methodological approach under consideration.

The case of the one-electron transfer can be generalized to include an $A^{n+}/A^{(n-m)+}$-type system. Here, n is the maximum ion valence at a change of its charge, m is the number of electrons transferred, and $n \geqslant m > 0$; $W_a = W_c + W_r$, $W_a = \alpha(me\eta)$, $W_c = \vartheta(me\eta)$, and $W_r = \chi(me\eta)$. The double cell $\{A^{n+},\ ne^-\}$ contains an extra ion A^{n+}, which diffuses in the solution at an arbitrary distance from the electrode, and charge ne^- from the metal surface.

An elementary event includes two stages: (1) cell formation (charging of the double vacancy as a capacitor) and (2) cell discharge (also as a capacitor). The total energy consumed by the external source to support the two stages is $W_s = me\eta$. The discharge has the form of the reaction

$$A^{n+} + me^- \to A^{(n-m)+}\,. \tag{4.3}$$

The electric capacitance of the cell $C = ne/\eta$ does not change during electron transfer. The cell charge Q drops from ne to $(n-m)e$ with a concomitant release of energy

$$W_c = \frac{1}{C}\int_{(n-m)e}^{ne} Q\,\mathrm{d}Q = me\eta\,\frac{2n-m}{2n}\,, \tag{4.4}$$

which is imparted to all the electrons being transferred. Therefore, one finds

$$\vartheta = \frac{W_c}{W_s} = 1 - \frac{m}{2n}\,. \tag{4.5}$$

Hence, there is a sequence of ϑ values, at $m = 1$ and $n = 1, 2, 3, 4, \ldots$:

$$\vartheta = 0.500;\ 0.750;\ 0.833;\ 0.875;\ \ldots \tag{4.6}$$

An overvoltage-charged double cell only gives out energy regardless of the direction of electron transfer (either cathodic or anodic). For an *external circuit*, the electron transfer in the cell is always a *discharge* to which formula (4.5) is applicable even if the equivalent circuit of the cell contains a serially connected microcapacitor and a microsource of the electromotive force simulating the difference between the electrode equilibrium potential and zero-charge potential (see Fig. 5).

The energy difference $W_s - W_a \approx W_s - W_c = (m/2n)me\eta$ is not used in the reaction and is removed from the interface (largely in the form of heat) either prior to the discharge or after it. Local currents and electrostriction are suitable but not the sole modes of conversion of the excessive energy difference into heat. *The loss of $W_s - W_a$ is independent of its specific mechanism*. The liberated heat cannot be used in the next discharge, in the first place because consecutive discharges are separated by a rather large spatial and temporal interval. The system does not accumulate the heat. The metal on which the discharge occurs maintains a constant temperature of the double layer.

Elementary nature of the transfer. Parameter α coincides with the apparent 'transfer coefficient' ζ (measured by experiment) only in a *one-stage process* which satisfies the following conditions: (1) the rate of charge transfer is determined by *one* stage (discharge or ionization), and (2) the product of this stage is an autonomous particle (the energy of its formation is independent of η which accounts for the coincidence of the decrease of activation energy and the increase of electron energy; in the case of hydrogen release, such a particle is H_3O). The effect of χ can be eliminated by reducing η; then, $\zeta = \vartheta$.

In the general case, n is the effective valence of a complex ion (either cation or anion) before the discharge or following ionization. Immediately after ionization, this valence may be higher than prior to the discharge due to the formation of ion pairs during the relaxation period. Direct and reverse processes in reactions involving multiply charged ions do not normally coincide. The corresponding coefficients α (α_d and α_b) near the equilibrium must satisfy the condition $\alpha_d + \alpha_b = 1$ which ensues from the Nernst equation for equilibrium potential. In case of a one-stage partial discharge of a multiply charged ion, α_d must be higher than 0.5 (at equilibrium $\alpha = \vartheta$). Then, $\alpha_b < 0.5$ which is not fulfilled in a single-stage process. Therefore, under certain sufficiently general conditions, the process opposite to the one-stage ion discharge is a multistage one, necessary to ensure dissipation of the excess energy.

According to the inequality $m[1 - (m/2n)] \leqslant n/2$, the energy $W_c = m\vartheta e\eta$ released by the cell is maximal at $n = m$: $W_{cm} = \max W_c = ne\eta/2$. *Prior to discharge*, the energy W_{cm} is *localized* in the cell as in a capacitor and determines the attractive force F_c between the ion and the metal. The constancy of cell effective capacitance *during the discharge* is a result of the exclusion of low-frequency constituents of permeability of the medium. The position of solvent molecules does not undergo any substantial change during electron transfer.

Energy dissipation associated with charging of a double-layer vacancy after the ion discharge is inherent in all electrolytic reactions and determines their kinetics. It has long passed unnoticed.

It accounts for the following characteristics of electrolysis:

(1) The energy of the double layer is distributed between autonomous elements, i.e. double cells.

(2) When a charged particle crosses the double layer, their interaction is limited by the cell's resource and energy inflow from the periphery.

(3) The energy spent for an elementary event of ion discharge is divided between the stages of valence modulation and charging of a double-layer vacancy.

(4) The charging stage following discharge of a univalent ion requires up to the half of the energy fed from an outside source.

5. Quantum insulation of discharge

During the discharge of a hydrogen ion, the contribution made by the cell undergoing the discharge (and completely insulated) is $\vartheta = 1/2$. The contribution of the periphery (χ) is responsible for the deviation of α from 1/2:

$$\alpha = \vartheta + \chi\,, \quad \chi \to 0 \quad \text{when} \quad \eta \to 0\,.$$

ϑ being known, χ can be found empirically by measuring α.

Measurements were performed by placing rectangular current pulses on the direct background current (Fig. 6). The difference between the electrode pulse potentials $\varphi_b(10)$ and $\varphi_b(1)$ was measured immediately after the pulses were discontinued at the maximum currents $10j_s$ and $1j_s$ including the background value $0.1j_s$, where $j_s \approx 0.1$ A cm^{-2}. This difference turned out to be equal to the overvoltage increment $\Delta_{10}\eta$ with a mean value of $\eta = 1.2$ V. It follows from Eqn (4.1) that $\alpha = (kT/e\Delta_{10}\eta)\ln 10$. The results of the experiment give $\alpha = 0.56 \pm 0.02$. Hence, $\chi = \alpha - 1/2 = 0.06 \pm 0.02$ at $\eta = 1.2$ V.

Discreteness of the double layer periphery. In the system under consideration, the ionic atmosphere has a compact structure for a large electron charge ($\eta > 1$ V). It is formed by a monolayer of cations H_3O^+ which are separated from the metal by solvate shells and give rise to equally-sized double cells (Fig. 7). Only that ion aggregate which shifts the electrode potential from equilibrium (shown in Fig. 7a) is essential for the kinetics. For this aggregate, η is the full potential jump in the ionic atmosphere. At any given moment, only an *insignificant fraction* of the double layer ions (of the order of 10^{-10} at the current density 1 A cm^{-2}) is involved in a discharge. Hence, the practically complete mutual *independence of elementary discharges* underlies Eqn (4.1) as the Boltzmann distribution (which is however inapplicable to *all the ions* of the double layer because of pronounced interion interaction).

A rise in η leads to a decrease of the distance between ions λ. In the case of a hexagonal arrangement of the ions, one finds

$$\lambda = \left| \frac{2z_0 e}{\sqrt{3}\eta\varepsilon_0\varepsilon_s} \right|^{1/2}. \tag{5.1}$$

Here, ε_0 is the electric constant and ε_s is the stationary relative permeability of the solution at $0 < z < z_0$, where z is the distance to the metal, and z_0 is the position of the ion center. For the system under consideration, $z_0 \approx 3$ Å, $\varepsilon_s \approx 7$, in compliance with the data on the double layer capacitance (0.2 F m^{-2}). It follows from (5.1) that $\lambda \approx 9$ Å at $\eta = 1.2$ V.

The classical value χ_0 of the contribution χ depends on the local potential jump η_r which would occur after a discharge at the ion's vacant site in the case of instantaneous effect of the periphery: $\chi_0 = \eta_r/2\eta$. In order to calculate η_r, the 'ions–

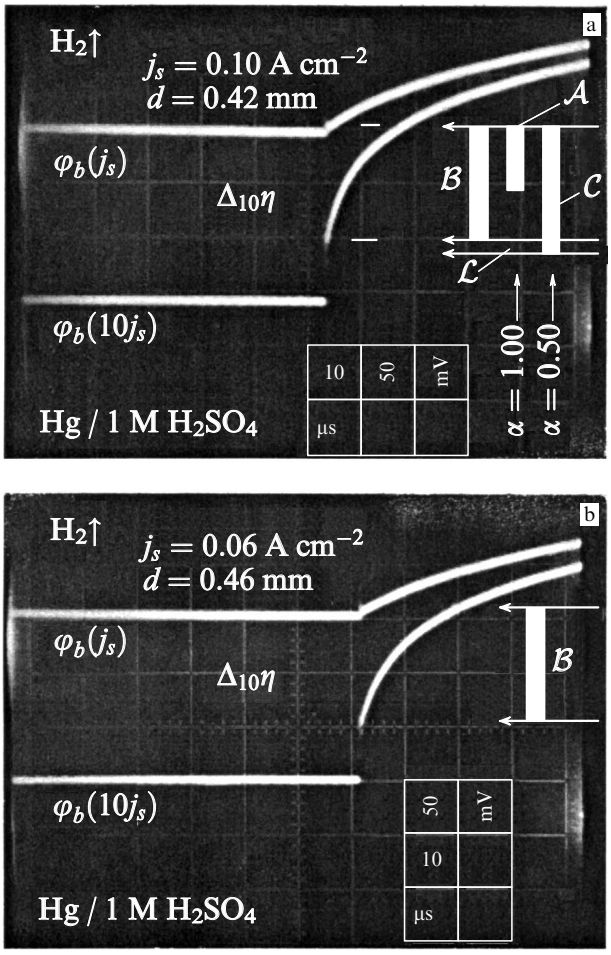

Figure 6. Contribution of the double layer periphery to the energy of the electron being transferred in a hydrogen ion discharge on mercury in an aqueous sulfuric acid solution: (a) effect of the degree of cell insulation on the differential overvoltage $\Delta_{10}\eta$. The height of the white rectangles shows the increment η for a ten-fold increase of the pulse current from $1\,j_s$ to $10\,j_s$: $\mathcal{A}$ — calculated at $\alpha = 1.0$ (macroscopic capacitor), $\mathcal{C}$ — calculated at $\alpha = 0.5$ (completely insulated double cell), $\mathcal{B}$ — measured as the difference between potential pulses φ_b of the auxiliary electrode on the portion where they fall after current pulses have been discontinued, $\mathcal{B} = 104$ mV, corresponding to $\alpha = 0.56$. The influx of energy from periphery causes $\Delta_{10}\eta$ to decrease by $\mathcal{L} = \mathcal{C} - \mathcal{B} = 12$ mV; (b) reproducibility of $\Delta_{10}\eta$ measured. Oscillograms were obtained from two consecutive mercury menisci of diameter d at the end of a capillary tube (inner diameter 0.3 mm) in an atmosphere of hydrogen; temperature 20°C.

metal' system is substituted by an equivalent 'ions–images' system in a homogeneous medium (short-lasting discharge). Summation is over a sufficiently large number of hexagonally arranged ions (in a circle of radius $100\,\lambda$). The η_r/η ratio is computed as a function of the parameter $\theta = \lambda/z_0$. Specifically, $[\theta, \eta_r/\eta]$ takes the following values:

[1, 0.733115], [2, 0.551015], [3, 0.425301], [4, 0.340666], [5, 0.282016], [6, 0.239708], [7, 0.208022], [8, 0.183523], [9, 0.164169], [10, 0.148276], [11, 0.135214], [12, 0.12424].

In the interval $0 < \eta < 2$, the result to within 2% can be approximated with the aid of the expression

$$\chi_0(\eta) = bc\sqrt{\eta}\left[1 - \exp\left(-\frac{a}{c\sqrt{\eta}}\right)\right], \tag{5.2}$$

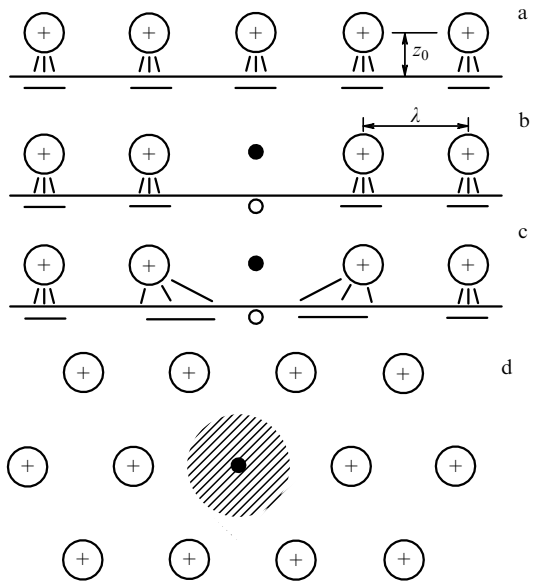

Figure 7. Double electric layer at the boundary between a metal and an electrolyte solution: (a) prior to ion discharge; (b, c) immediately after discharge with (c) and without (b) a quantum of energy incoming from the periphery; (d) double vacancy region (hatched) surrounded by peripheral ions. Double vacancy components [ion (•) and electron (○) sites] and field lines of force are shown schematically.

where $a = 0.680$, $b = 0.741$, $c = |\sqrt{3}\varepsilon_0\varepsilon_s z_0/2e|^{1/2}$; η, and c are measured in units of V and V$^{-1/2}$, respectively. The calculation of $\chi_0(\eta)$ using Eqn (5.2) yields $\chi_0(1.2\text{ V}) = 0.22$ which is significantly (almost 4-fold) higher than the measured value 0.06.

Discreteness of energy transfer. Classical computations give the following average time of charge transfer in a double cell:

$$\tau_r = z_0\sqrt{\frac{2m_0}{(\vartheta + \chi_0)e\eta}}, \tag{5.3}$$

where m_0 is the rest mass of the charge. At $\eta = 1.2$ V, the electron transfer takes $\tau_r = 1.09 \times 10^{-15}$ s, and the classical energy influx from the periphery is $W_{r0} = \chi_0 e\eta = 0.264$ eV. The product of these two values leads to the inequality

$$W_{r0}\tau_r \approx 2.9 \times 10^{-16}\text{ eV s} < \hbar = 6.5822 \times 10^{-16}\text{ eV s}, \tag{5.4}$$

here $\hbar$ is Planck's constant. It is opposite to the condition $W_{r0}\tau_r \gg \hbar$ in which the classical value of W_{r0} coincides with the true energy influx. Quantum effects are essential, whereas the effect of relativistic delay is insignificant.

The recorded electric current is generated only by cells undergoing discharge. Similar to the cell discharge, the release of self-energy W_c is here a *certain* event. The energy inflow W_{r0} from the periphery is an *accidental* event. It may (Fig. 7c) or may not occur (Fig. 7b). In the quantum context, the two events do not interfere (i.e. their amplitudes are not summed). Hence, it is an objective necessity to distinguish a double cell as an autonomous element and subdivide the energy into internal and external. The interaction between the cell and the periphery may be regarded as a transition from an unstable isolated state to a stable one with the absorption of the quantum energy $W_{r0} = \chi_0 e\eta$. In conformity with Ref [23],

the mean lifetime of the isolated state may be represented as

$$\tau_c \approx \frac{\hbar}{W_{r0}} = \frac{\hbar}{\chi_0 e\eta} \,. \tag{5.5}$$

Comparison with the time of charge transfer (τ_r) gives

$$\frac{\tau_r}{\tau_c} = \chi_0 \frac{z_0}{\hbar} \sqrt{\frac{2m_0 e\eta}{\vartheta + \chi_0}} . \tag{5.6}$$

The probability Ξ that the cell remains insulated till the discharge is completed can be found from the Poisson distribution [24] as $\Xi = \exp(-\tau_r/\tau_c)$. Accordingly, the probability of energy inflow from the periphery for time τ_r is $\Theta = 1 - \Xi$ or

$$\Theta = 1 - \exp\left(-\frac{\tau_r}{\tau_c}\right) . \tag{5.7}$$

The mean contribution of the periphery

$$\chi = \chi_0 \Theta = \chi_0 \left[1 - \exp\left(-\frac{\tau_r}{\tau_c}\right)\right] . \tag{5.8}$$

In the experiment described above, $\tau_r/\tau_c = 0.44$, $\Theta = 0.36$ at $\eta = 1.2$ V. The calculation gives $\chi = 0.08$ which is close to the experimentally found value $\chi = 0.06$. One of the consequences is the elucidation of the nature of the transferred charge, it being an electron rather than a proton which is three orders of magnitude heavier. In the case of proton transfer, $\tau_r/\tau_c = 19$, and the effect of quantum insulation is practically absent.

In the more general case, when a cation with the valence n acquires m electrons, one finds

$$\chi_0 = \frac{m}{2n} \frac{\eta_r}{\eta}$$

for the classical energy influx from the periphery $W_{r0} = m\chi_0 e\eta$.

6. Photoemission of secondary electrons

The notion of the work function introduced by A Einstein in 1905 [25] to explain the photoeffect has become of paramount importance in the theory of contact potential difference. Measurements of the photoemission threshold in vacuum agree with the results obtained by the method of vibrating capacitor. The difference between work functions for zinc and copper (0.2 eV) is small compared with the potential difference in solutions of their own ions (1.1 V).

Studies of photoemission from metals into solutions include observation of the effect of potential jump in a double layer on the amount of work that the electron must produce on leaving the solid body [26]. In order to take this effect into consideration, the Einstein equation was expanded by introducing the term $e\eta$:

$$E_{\text{kin}} = \hbar\omega - \hbar\omega_0 + e\eta \,, \tag{6.1}$$

where E_{kin} is the kinetic energy of the emitted electron, ω is the circular emission frequency, and ω_0 is the frequency threshold. The dependence of the photocurrent on the potential is measured at a given ω. The threshold potential η_t is found by the extrapolation of the photocurrent to zero. It corresponds to the condition $E_{\text{kin}} = 0$. It follows from Eqn (6.1) that

$$\frac{\partial(\hbar\omega)}{\partial(e\eta_t)} = -1 \,. \tag{6.2}$$

The rough agreement between (6.2) and the experimental data is considered to confirm the theory [26]. However, Eqn (6.2) also satisfies a more general equation

$$E_{\text{kin}} = \upsilon(\hbar\omega - \hbar\omega_0) + \alpha e\eta \tag{6.3}$$

with $\upsilon \approx \alpha$. Both the length and the time of the electron range in a double layer are of the same order of magnitude as during an ion discharge (several angstroms, 10^{-15} s). The classical peripheral energy is unavailable for the electron during this time. Its loss is not less than during a normal cell discharge (see Section 5). Under such conditions, the electron may receive maximum energy from the double layer when it escapes the metal through a double cell, i.e. as a result of ion discharge. Simultaneously, the work function decreases by $\alpha e\eta \approx e\eta/2$ and $\upsilon \approx \alpha \approx 1/2$. Therefore, it follows from Eqn (6.3) that the photocurrent is due to secondary electrons which receive part (υ) of the photon energy in collision with primary electrons [27].

The difference between a macroscopic potential jump η in a double layer and a local jump at the site of charge transfer has a remote analogy in hydrodynamics. The velocity of fluid outflow through a hole in the flat bottom of a vessel depends on the total fluid level while it remains much greater than the hole diameter. The outflow from a thin layer is a function of the local fluid level which is either zero or considerably lower than the general one.

7. Spontaneous condensation of ionic atmosphere

The dependence of the electric potential φ on the spatial charge density ρ is usually described by the Poisson equation

$$\Delta\varphi = -4\pi\rho \,. \tag{7.1}$$

S Poisson was the first to derive this equation in 1813 for the solution of gravity problems based on Newton's law. He introduced an additional term with the distributed mass ρ into the Laplace equation.

In 1824 and 1826, Poisson proposed two variants of this equation, $\Delta\varphi = -2\pi\rho$ and $\Delta\varphi = -4\pi\rho$, the former related to the outer surface of an attracting body A, and the latter to its inner region [28]. These equations are valid on the condition that the body, 'le corps A', can be represented as "un très-grand nombre de parties, dont les dimensions extrêmement petites eu égard à celles de ce corps..." — a very large number of parts, the dimensions of which are infinitely small compared with the size of the body ([28], p. 450). Subsequent applications of the Poisson equation to electrical phenomena have been based on the analogy between the Newton and Coulomb laws.

The expression for the force F_a acting on an elementary charge e along the axis z in a field with the potential φ is

$$F_a = \frac{e\partial\varphi}{\partial z} \tag{7.2}$$

which is equivalent to Newton's second law where, in a given case, the mass is multiplied by the acceleration due to gravity $g = \partial\varphi/\partial z$. The equation for ion diffusion at a concentration

c_i has the form

$$\frac{\partial c_i}{\partial z} + \frac{F_a c_i}{kT} = 0 .$$

Substitution of Eqn (7.2) into this equation gives a ratio resembling the Boltzmann distribution

$$c_i = c_{i0} \exp\left(-\frac{e\varphi}{kT}\right), \tag{7.3}$$

where c_{i0} is the ion concentration in the solution volume. Equations (7.1)–(7.3) provide the basis for the classical approach to the theory of the ion double layer at the metal–solution interface.

In the Poisson equation (7.1), the potential φ is a function of *all* charges including the ion of interest. In Eqn (7.2), this ion is under effect of potential φ which *it actually creates itself*. Unlike a stone the size of which is negligibly small compared with that of the Earth (and which therefore does not influence the acceleration caused by gravity), the contribution of an ion of a discrete double layer to the potential change is close to the half of this change, in rough analogy to the contribution of one plate of a capacitor to the total change created by its two plates. Although Eqns (7.2), (7.3) are inapplicable under these conditions, they are used all the same.

In the case of a weak discharge current, the double layer behaves as a capacitor free of leakage and having a diffuse structure. The theory of the diffuse double layer was proposed by G Gouy in 1910 [29] and independently by D Chapman in 1913 [30]. The two authors used equations (7.1) and (7.3) as a basis and interpreted the latter as the Boltzmann distribution. Further modifications of this theory [31] left its basic principles unaltered. The theory gives the effective thickness of the ionic atmosphere, i.e. the gap between the plates of a flat capacitor which is equivalent to the double layer in terms of capacitance. Later (in 1923), a similar expression was obtained by P Debye and E Hückel [32] for the charged atmosphere surrounding an ion in their theory of electrical conductivity of solutions. Today, it is known as the Debye screening radius.

Charge continuity and dilution. Gouy and Debye's theories differ in terms of geometry. The former theory examines a charged plane (electrode), while the latter is concerned with a point charge (ion). The central ion potential *falls* rapidly with the distance to a value which is small considering the thermal motion of the surrounding ions. This prompted Debye to use the Boltzmann distribution as the first approximation (the exponent is expanded into a series).

Opposite conditions occur at the boundary between a metal and a solution. The potential of the electrode as a charged plane *grows* linearly with increasing distance. The potential energy of the ions is high compared with the energy of their thermal motion. Gouy did not consider the applicability of the Boltzmann distribution to such a boundary. Nor was this problem discussed by later authors, probably because there was no other way to its solution.

Let us watch the behavior of the double layer in the course of diluting a solution. Suppose that it was first charged through the external circuit. Then, the current was disconnected (the charges of both the metal and the ionic atmosphere were fixed in magnitude), the metal coated with a film of the initial solution was transferred into a fresh solvent, and the solution underwent natural dissolution owing to diffusion. According to the classical theory, a decrease of the solution concentration to zero results in an infinite increase of the double layer thickness (and the Debye radius). In the experiment under consideration, this would mean that *all the ions* go away to infinity through diffusion against a *constant* (for the nearest ions) *force of attraction* to the charged metal which generates a uniform field. This is known to be impossible. The outflow of ions from a charged metal is dictated by Eqn (7.3), that is $c_{i0} \to 0$ leads to $c_i(\varphi, z) \to 0$ at any finite φ and z. This discrepancy indicates that a different approach is needed to the double layer theory.

Critical potential. Because the classical theory postulates the removal of all the ions to infinity, there must operate a so far inexplicable mechanism which brings them back to the charged metal. Calculations based on *first principles* have demonstrated that the ions really come back after a certain critical potential change in the double layer is reached. This critical potential change does not depend on the concentration of the solution, which allows this phenomenon to be regarded as a spontaneous condensation of the ionic atmosphere.

The central point of the novel approach is the expression for the force of ion attraction in the double layer. It ensues (without rigorous derivation) from double cell properties. The criterion of its validity is experimental findings. The maximum energy $W_{cm} = ne\eta/2$ stored in a cell $\{A^{n+},\ ne^-\}$ $(n > 0, \eta > 0)$ corresponds to the force of interaction between its charges:

$$F_c = n\frac{e\eta}{2z}, \tag{7.4}$$

that is the mean force with which an extra ion at a distance z from the charged metal surface is attracted to it. The substitution of this force into a system of diffusion equations gives a desired charge distribution in the discrete ionic atmosphere and also the double layer capacitance as a function of the potential jump [33]. Components undergoing diffusion include (1) excessive cations (e.g. Na^+ in the vicinity of the negatively charged metal), and (2) neutral cation–anion groups (e.g. dissociated salt $NaF \to Na^+ + F^-$) which remain on the whole unaffected by the metal's field. For the purpose of computation, there is no need to indicate which concrete cations are excessive. This explains why Eqn (7.4) retains sense for any concentration of the solution.

Equations for the discrete ionic atmosphere. When cations are present in excess (for definiteness), the system in dimensionless variables has the form

$$\frac{\partial}{\partial y}\left(\frac{\partial u}{\partial y} + x\frac{u}{y}\right) - vu = 0, \tag{7.5}$$

$$\frac{\partial^2 v}{\partial y^2} + \frac{n_-}{n_- - n_+}\, vu = 0, \tag{7.6}$$

where u and v are the molar concentrations of excessive cations and neutral groups, respectively, counted per molar concentration c_0 of the electrolyte in a solution volume, $x = ne\eta/2kT$ is the potential jump in the ionic atmosphere, $y = a(z/\zeta z_0 + 1 - 1/\zeta)$ is the distance from the metal surface ($y = a$ at $z = z_0$), $\zeta = \varepsilon_v/\varepsilon_c \geqslant 1$ for $x = 0$, ε_c and ε_v are permeabilities of the solution in the ranges $0 < z < z_0$ and $z_0 < z < \infty$, $n_- < 0$ and $n_+ = n > 0$ are the anion and cation valences with the greatest common measure $\rho_m \geqslant 1$, and finally

$$a = \zeta z_0 e\sqrt{\frac{n_- n_+ (n_- - n_+) N c_0}{\rho_m \varepsilon_0\, \varepsilon_{vm}\, kT}}, \tag{7.7}$$

where N is the Avogadro number, and $\varepsilon_{v\mathrm{m}} = \max \varepsilon_v$ (in the solution volume). When the potential is sufficiently large ($x \geqslant x_v$), the condition $u(x,a) \gg v(x,a)$ is fulfilled (i.e. the predominance of excessive cations near the surface of the electrode). Then, Eqn (7.5) may be considered to contain $v = \mathrm{const} = v(\infty, a)$ and solved separately. The distribution of the excessive charge $u = u(x,y)$ found in this way leads to the expression for the dimensionless integral capacitance G_i of the double layer as a function of the potential x at different solution concentrations (Fig. 8a):

$$G_i(x,a) = \frac{a \int_a^\infty y^{(1-x)/2} K_{(1+x)/2}(y)\,\mathrm{d}y}{\int_a^\infty y^{(3-x)/2} K_{(1+x)/2}(y)\Phi(sax/y)\,\mathrm{d}y}\,, \tag{7.8}$$

where $K_\upsilon(y)$ is a Bessel function of the order υ, the function $\Phi(sax/y)$ describes the field effect on the permeability of the solution; $\Phi \approx 1$ if this effect is weak (this condition is normally fulfilled at $x < 3$), s is the parameter reciprocal to the threshold field strength E_m at which the rate of decrease ε_v with the field growth is maximal (the results of the above experiments agree with the value $E_m = 3.2 \times 10^8$ V m^{-1} to which $s = 0.25$ corresponds).

It follows from the theory developed by L Onsager that [16]

$$\Phi(X) = b\,\frac{1}{1 + 3(b-1)(1/X)(\coth X - 1/X)}\,,$$

where b characterizes a decrease of the permeability at the maximum field intensity attainable in experiment.

The dimensionless differential capacitance of a double layer is given by the equality $G_d = G_i + x\,\mathrm{d}G_i/\,\mathrm{d}x$. Dimensional capacitances are $C_i = (\varepsilon_0 \varepsilon_{vm}/\zeta z_0) G_i = |q/\eta|$, $C_d = (\varepsilon_0 \varepsilon_{vm}/\zeta z_0) G_d = |\,\mathrm{d}q/\,\mathrm{d}\eta|$. The limiting curve $G_i(x,0)$ with $a = 0$ has a slope on which the finite concentration curves $a = 1$ (10^{-2} M), 0.1 (10^{-4} M), ... ([M] = mol l^{-1}) lie. This slope restricts the half-width of the capacitance minimum by the critical potential

$$x_c = 2\,, \quad \eta_c = 4\frac{kT}{ne}\,, \tag{7.9}$$

$$G_i(x,0) = 1 + (1-x)^{-1} \text{ at } x \geqslant 2\,, \tag{7.10}$$

$$G_i(x,0) \equiv 0 \quad \text{at } x < 2\,, \tag{7.11}$$

with $\eta_c = 0.1$ V for $n = 1$ and $T = 273$ K.

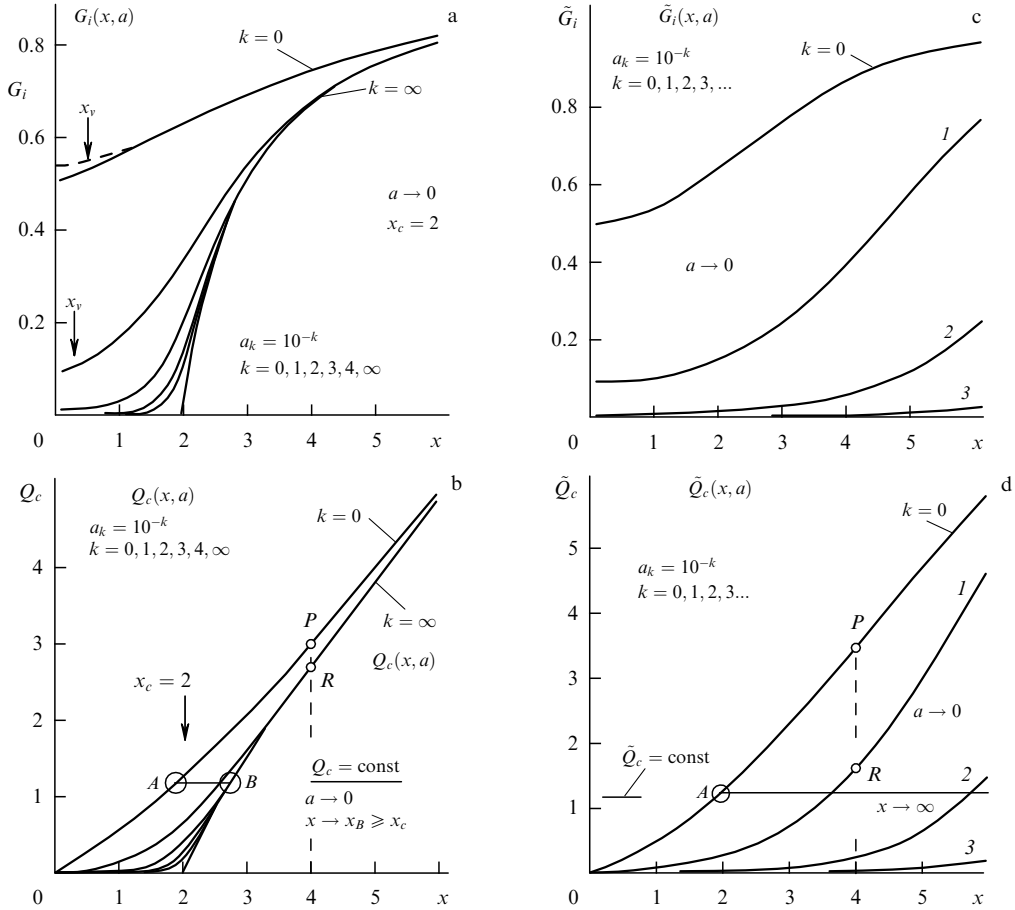

Figure 8. Integral capacitance G_i and charge density $Q_c = xG_i$ of the double layer as a function of the potential x during spontaneous condensation of the ionic atmosphere at different concentrations a^2 of the solution (a, b), $C_{i,d} = (\varepsilon_0 \varepsilon_{vm}/\zeta z_0) G_{i,d}$, $\eta = 2xRT/nF$; $C_{i,d} = (0.24\ \mathrm{F\,m^{-2}})\,G_{i,d}$, $\eta = x \times 0.05$ V at $n_+ = -n_- = 1$, $\varepsilon_{vm} = 80$, $z_0 = 3 \times 10^{-10}$ m, $\zeta = 10$, $T = 293$ K, $a = a_k$. For comparison, the integral capacitance $\tilde{G}_i$ and charge density $\tilde{Q}_c$ are calculated for the same conditions in terms of the classical theory (c, d). At $Q_c = \tilde{Q}_c = \mathrm{const} = 1.2$, the real rise in the potential x during dilution ($a \to 0$) is limited by the segment AB (b), whereas in the classical theory such a segment beginning from A has no end which implies an infinite potential growth during dilution (d).

Under the same conditions, the classical expression for the integral capacitance has the form (Fig. 8c):

$$\widetilde{G}_i(x,a) = \left(1 + \frac{x}{a \sinh x}\right)^{-1}. \qquad (7.12)$$

Unlike the classical theory and its modifications, Eqn (7.8) describes the following properties of the double layer: (1) above the critical potential the capacitance remains finite as the concentration falls to zero, and (2) for any fixed charge the potential increment in the course of dilution is restricted by a critical value ($x_c = 2$, $\eta_c = 0.1$ V instead of classical infinity, Fig. 8b,d). In a concentration range from 10^{-2} to 10^{-4} M, the classical potential growth is twice or more than the real one depending on the charge value. At $x = 0$ (zero charge point), Eqns (7.8) and (7.12) give similar results.

The differential capacitance G_d (or $G_i + x\partial G_i/\partial x$) is measured in the alternating current regime. The calculated curves intersect at the inflection point near the critical value $x_c = 2$, $\eta_c = 0.1$ V (Fig. 9a,b). Therefore, the width of the differential capacitance minimum remains constant on dilution. This asymptotic property is satisfied at concentrations below 0.1 M.

The results of experiments with 10^{-2} and 10^{-3} M solutions indicate that the coordinate of the capacitance inflection point (minimum half-width) equals the critical potential to within 20% though the equation $\eta_c = 4kT/ne$ is derived using no adjustable parameters whatever.

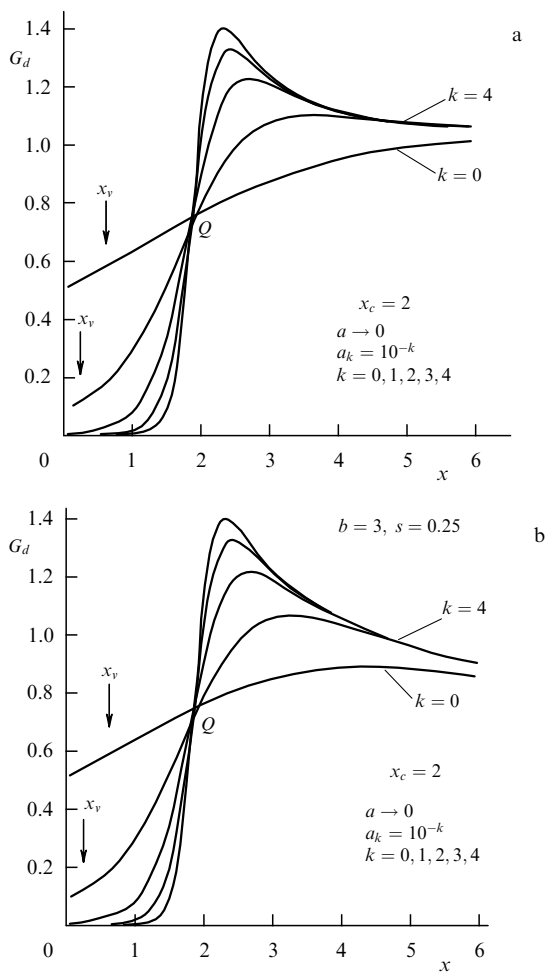

Figure 9. Differential capacitance G_d of the double layer as a function of the potential x at different concentrations a^2 of the solution: (a) in the absence of the field effect on the dielectric constant of the solution ($\Phi \equiv 1$), (b) under the effect of the field. The curves intersect practically at a common inflection point corresponding to the critical potential, regardless of the concentration below 0.1 M. Conditions are the same as in Fig. 8.

The agreement of this equation with the experimental results is of interest in that its right-hand side contains only fundamental physical constants: the charge quantum e and the Boltzmann constant k, besides the temperature T and integer n. The left-hand side includes a *single special parameter* η_c of the double layer, which may be measured with a sufficient accuracy. This suggests a quantum origin of the capacitance minimum and the validity of Eqn (7.4): in a diffuse double layer, the force of attraction of an extra discrete charge to the interface decreases in inverse proportion to the distance from it.

The practical value of Eqn (7.4) is due to the fact that it provides a simple and independent tool for the description of the double layer at the boundary between a solution and a metal, biological membrane or other immiscible liquid. For a given potential jump at the boundary, there must be a certain relationship between the distance and the average force of attraction of the discrete charge. This inference does not contradict the principle of energy conservation and is confirmed by experiment. The potential given, this excludes an independent contribution of the image for the same reason as between two plates of a capacitor.

Pulse growth of the surface. Another result of spontaneous condensation, i.e. the asymptotic independence of a double layer charge of the concentration during potential enhancement in the supracritical region ($x > 2$, $\eta > 0.1$ V), can be just as well verified experimentally equally with the correspondence between the capacitance minimum and critical potential. Specifically, this is feasible for concentrations 10^{-2} and 10^{-4} M (see the curves with parameters $a = 1$ and $a = 0.1$ in Fig. 8).

For these concentrations, the new and classical theories give quite different charge ratios when the potential $x = 4$ ($\eta = 0.2$ V). On the charge versus potential curves (Fig. 8 b,d), points with $x = 4$ are marked as $P(a = 1,\ c = 10^{-2}$ M) and $R(a = 0.1,\ c = 10^{-4}$ M). The $Q_c(R)/Q_c(P)$ ratio is 0.91 and 0.46 in the new and classical theories, respectively. Direct experimental measurements of the double layer charge in strongly diluted solutions (10^{-4} M and lower) are lacking from the scientific literature because they are difficult to perform by traditional methods.

A simple solution to this problem consists in the use of pulse interface growth. In a time of 0.1 s upon injection of a known amount of mercury, its meniscus expands from the capillary channel into a stationary drop (Fig. 2b). The current charging the drop up to a desired initial potential is recorded during and after its growth (Fig. 10). The charge to be found is equivalent to the area under the curve of current versus time (barring a relatively small residual current which is estimated from the difference between the ordinates of the beginning and end of the oscillogram).

Based on the above experimental data, the charge ratio for 10^{-4} and 10^{-2} M solutions at $\eta = 0.2$ V was found to be 0.8. This value suggests the existence of a spontaneous condensation effect which substantially weakens or totally eliminates (in the limit) the influence of the concentration.

The ratio thus found is significantly greater than the charge ratio predicted by the classical theory. At a higher potential $\eta = 0.5$ V, the electrode charges measured in 10^{-4} and 10^{-2} M solutions are practically identical (9 μC cm^{-2}).

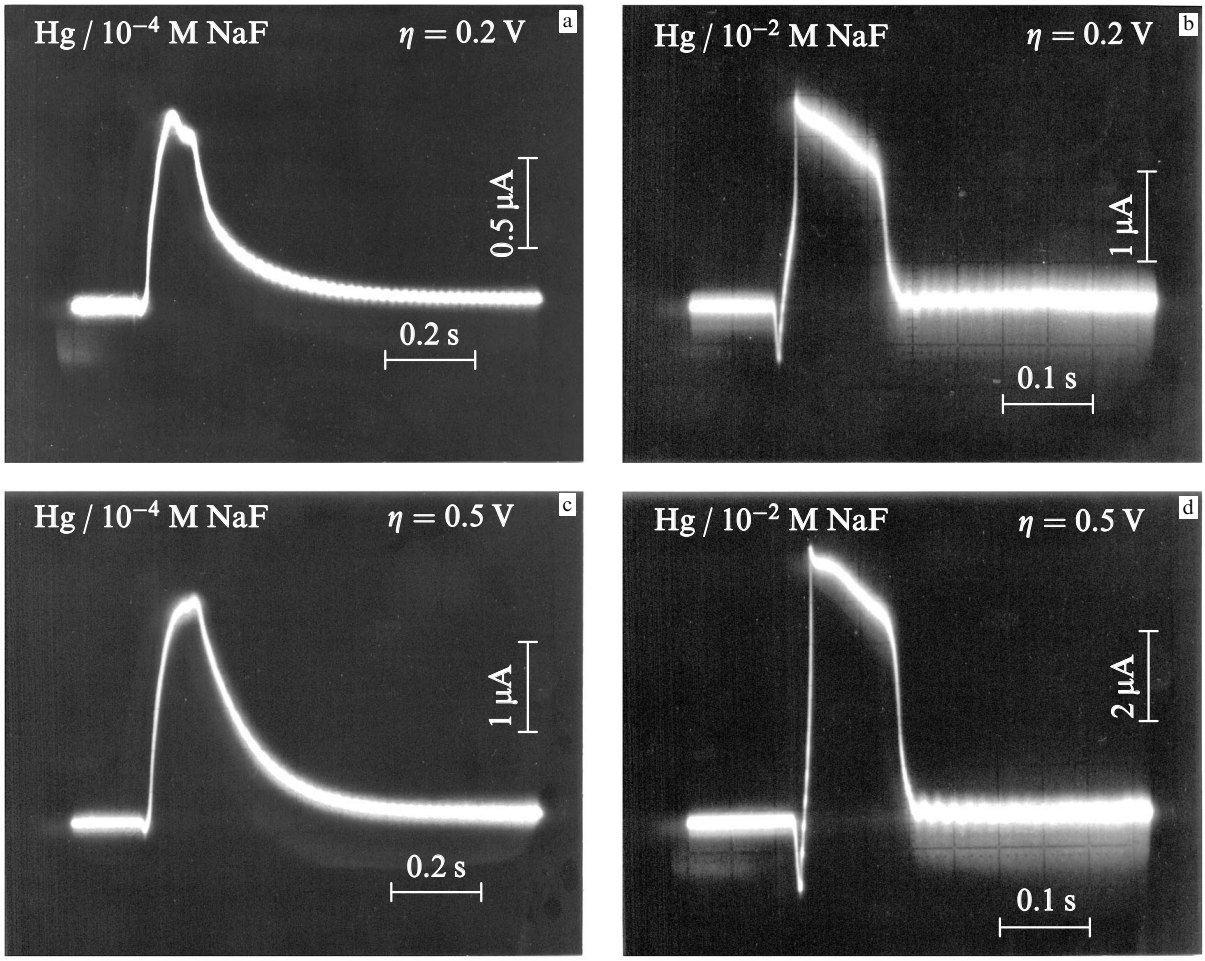

Figure 10. Current versus time oscillograms obtained in an experiment on the pulse growth of the mercury electrode surface in 10^{-4} (a, c) and 10^{-2} M (b, d) aqueous NaF solutions at 0.2 and 0.5 V from the zero-charge potential in the cathodic direction. Opposite two-fold changes of the current and time scales do not affect the area scale, which allows for direct comparison of the charges. The growth proceeds from the meniscus in a capillary channel 0.4 mm in diameter to a 1.2-mm high drop in the form of a spherical segment with diameter 1.5 mm and open area of 5.8 ± 0.1 mm^2, at 20 °C in an atmosphere of argon. The negative current burst is induced by the initial shrinkage of the meniscus.

8. Adsorption steps under exclusion of wave function nodes

The hydrogen problem in Volta's element was a focus of interest for many researchers. Humboldt described an experiment on the contact of two metals in an aqueous solution and gas release on one of them in 1797, after he had visited Volta's laboratory. Long exploitation of the battery led to the accumulation of gaseous hydrogen and enhanced the internal resistance of the source. J Joule proposed using a rotating electrode to prevent this effect.

Ritter's studies of 1803 showing the possibility of accumulating electricity by electrolysis were extended by W Grove in 1839 to the investigation of back current following electrolysis which was accompanied by the liberation of hydrogen and oxygen in a vessel with platinum electrodes [34]. The accumulator was closed with respect to reagents. Grove's system differed from others in that it allowed feeding gaseous and nongaseous substances from an outside source. This prompted a new mode of generating electricity by bringing 'fuel' in direct contact with electrodes. Their interaction proved to be much more economical than mere burning hydrogen in oxygen. A similar principle of energy conversion is realized in living creatures. The first experiments with fuel elements date to the early 20th century. Today, they are considered to be the most promising and ecologically friendly sources of energy with an efficiency as high as 70%. The main property of the material of electrodes is considered to be the ability to adsorb atomic hydrogen because the breakdown of a hydrogen molecule facilitates its ionization by the back current.

The importance of adsorption for electrolysis was mentioned in Maxwell's *Treatise*: "Of course these bubbles, by preventing the fluid from touching the metal, diminish the surface of contact and increase the resistance of the circuit. But besides the visible bubbles it is certain that there is a thin coating of hydrogen, probably not in a free state, adhering to the metal, and as we have seen that this coating is able to produce an electromotive force in the reverse direction, it must necessarily diminish the electromotive force of the battery" [2, § 272].

Model of an inhomogeneous monolayer of two sorts of atoms. In adsorption studies, it is easier to examine the transformation of hydrogen ions in a solution to adsorbed atoms. Such surface charging occurs prior to the release of gaseous hydrogen and is a nonmonotone process. In case of a linear change of the potential on platinum, the charging current goes through two consecutive maxima

[35] regardless of the crystallographic orientation of the surface.

The interpretation of this phenomenon has changed little during the last 50 years [36]: "It is well known that H-atom electroadsorption on Pt results mainly in the formation of two different adsorbates, namely, the weakly and strongly adsorbed H-atom" (1996). According to the generally accepted interpretation, a metal surface harbors two sorts of sites. First, the sites of one sort (parterre) are filled, then those of the other (dress circle). After the entire surface is occupied ('the theatre is full already...')†, it carries two readily distinguishable varieties of adsorbed atoms. In Ref [36], the composition of the hydrogen monolayer on Pt (100) was calculated by the molecular orbital method. The layer was found to contain H atoms in the following proportion: only about half (7/16) of the external platinum atoms were covered by H atoms whereas the remaining H atoms were located in surface depressions and bound to the inner Pt atoms; as a result, the other half of the external Pt atoms remained unoccupied.

As frequently happens, the inferences of this theory appeared to be predetermined by the universally accepted standpoint. However, experimental findings indicate that all the external platinum atoms, rather than half of them, are equally covered with hydrogen atoms arranged in a monolayer.

Additional data on hydrogen adsorption were obtained independently in studies concerning the effect of this process on the surface tension of platinum, iridium, and rhodium [14, 37, 38]. Rolled and annealed platinum and rhodium sheets and foils with the surface orientation (100) were used in these experiments, in agreement with the amount of hydrogen adsorbed in the monolayer and the surface reproducibility following anodic oxidation with recrystallization after oxide cathodic reduction. Figures 11–13 show oscillograms obtained in these experiments: $\partial\gamma/\partial q - E$, $|\partial\gamma/\partial q| - E$, $\partial\delta/\partial q - E$, where γ is the surface tension of the solid electrode (Pt, Rh), $\delta = V/S_e$ is the effective thickness of the electrode including variable thickness of the adsorbed layer, V is the volume of the electrode–solution system, S_e is the true electrode area, $q = Q/S_e$, Q is the charge imparted to the electrode, and E is the electrode potential in relation to the equilibrium hydrogen electrode.

Uniform stepwise elongation of the adsorption bond. The two current density (j) maxima of hydrogen adsorption on platinum coincide, on the axis of potentials, with the two minima of the surface tension derivative $\partial\gamma/\partial q$ (Fig. 11, T_{21} and T_{10} at $E_{21} = 0.25$ V and $E_{10} = 0.13$ V). The reaction $H^+ + e^- \rightarrow H_{ad}$ can be slowed down by a rise in the current frequency and cooling. For 10 kHz and −29 °C (Fig. 11b), the *variable constituent* of the hydrogen atom inflow from the solution towards the surface is greatly reduced which is practically equivalent to its elimination. However, the surface tension oscillogram still shows two minima. This suggests that they reflect transitions between hydrogen states which occur *within the surface itself*. Two transitions, T_{21} and T_{10}, are made between *three* states of an adsorbed hydrogen atom: H(2), H(1), H(0), in increasing order of filling. Similar processes can be observed in iridium (two transitions) and rhodium (one transition T_{10}, Fig. 11c). The data on surface tension are at variance with the 'two sorts model'.

† The author appears to allude to the popular stanza 20 in Chapter 1 of 'Yevgeny Onegin', the novel in verse by Aleksandr Pushkin. (*Translator's note*.)

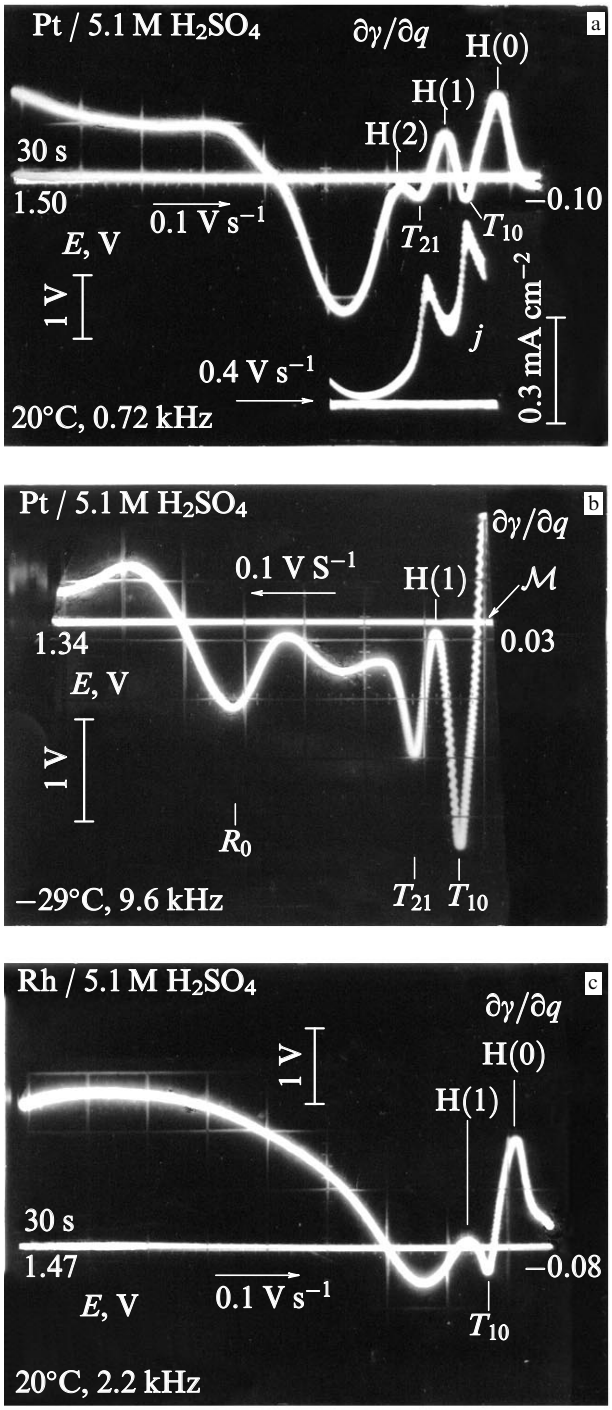

Figure 11. Effect of stepwise narrowing of the wave d-function of a metal atom with increasing double-layer field during hydrogen adsorption. The relationship between the number of internal nodes of the function (two on platinum and one on rhodium) and the number of surface tension derivative ($\partial\gamma/\partial q$) minima ($T_{21}$ and T_{10}) during hydrogen adsorption from a sulfuric acid solution on platinum (a, b) and rhodium (c). Surface orientation (100); linear change of the electrode potential E [relative to the equilibrium hydrogen electrode (EHE)]; j is the hydrogen ion discharge current density. Fluctuations of the electrode charge density q are determined by alternating current of frequencies shown at the bottom of each diagram. Exposure is 30 s at the initial potential (a, c). $\mathcal{M}$ shows the change in the slope upon reaching the monolayer.

The electrocapillary expansion method [37] was used to record ultrasound emitted from the platinum surface covered with adsorbed hydrogen (see Fig. 13). An alternating current

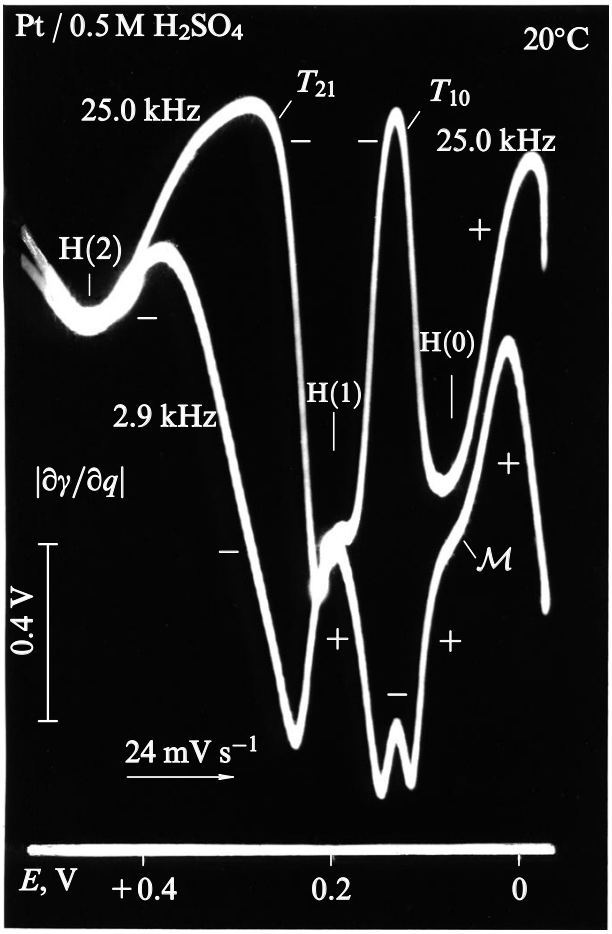

Figure 12. Surface tension derivative $|\partial\gamma/\partial q|$ for platinum at two frequencies of alternating current at a time and for a single scan of the platinum electrode potential E in the area of hydrogen adsorption from diluted sulfuric acid; surface orientation (100). Alternation of frequency-dependent and independent sections: H(2), H(1), H(0) — independence; T_{21}, T_{10} — dependence; E — in the EHE scale. The diagram shows the signs and the site $\mathcal{M}$ where the monolayer is reached.

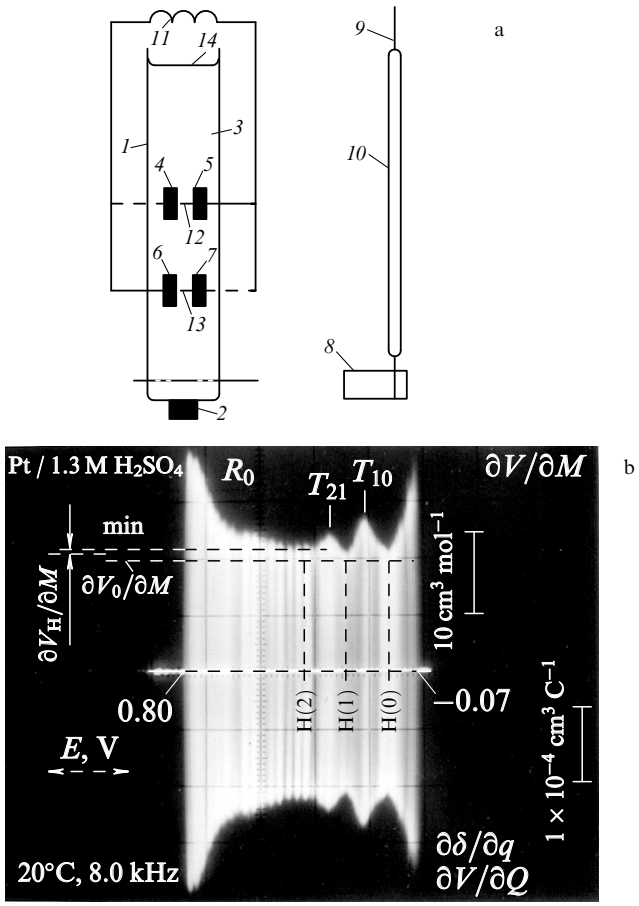

Figure 13. Effect of stepwise elongation of the wave d-function of a metal: (a) measuring device; (b) extrema of the interface thickness derivative with respect to the charge density $\partial\delta/\partial q$ as a function of the potential E (EHE scale) in the course of hydrogen adsorption on platinum. Surface orientation (100); *1* — vessel, *2* — piezoelement, *3* — solution, *4*, *5*, *6* and *7* — pairs of electrodes from the metal of interest (platinum), *8* — plate of each electrode, *9* — current terminal, *10* — glass tube, *11* — secondary coil of the transformer, *12*, *13* — displacement nodes of the solution, *14* — solution level in the vessel. $\partial\delta/\partial q = \partial V/\partial Q \approx -(\partial V/\partial M)/F$, where M is the amount of adsorbed hydrogen, F is the Faraday number, $\partial V_0/\partial M \approx$ const is the background due to displacement of the solution center of mass during the passage of an alternating current, $\partial V_{\mathrm{H}}/\partial M \approx$ const is the volume increment contribution under a hydrogen ion discharge.

was passed between two electrodes placed in adjacent displacement nodes. Double pressure fluctuations were sensed by a piezoelement under the vessel bottom. Thermal expansion of the solution caused by the passage of alternating current between the two electrodes in one displacement node served as a standard. Using this method, changes in the volume of the adsorbed hydrogen layer were measured. If referred to a part of the surface filled at a peak potential of each transition (E_{21} and E_{10}), these vibrations gave the elongation steps of the electron cloud which supported the Pt – H bond. The two steps turned out to be virtually identical, 0.2 Å each.

The shape of the surface tension curves in the hydrogen adsorption region did not change with increasing H_2SO_4 level from 1 to 18 M (practically in the absence of water), which indicated the absence of the distortion effect of the solution.

Nonoverlapping steps. The effect of current frequency is especially striking (see Fig. 12). The curves $|\partial\gamma/\partial q| - E$ obtained at two frequencies (2.9 and 25.0 kHz) *at a time* show frequency-independent intervals alternating with strongly frequency-dependent intervals. This is an important experimental finding which uniquely suggests the absence of an overlap between H(2) – H(1) and H(1) – H(0) transitions *separated* by frequency-independent intervals. This indicates that the transitions are complete within frequency-dependent intervals. The completeness of the transitions implies a homogeneous state of all adsorbed atoms before and after the transition: that is only state H(2) is feasible in the first independent interval (in the vicinity of $E = 0.45$ V), only state H(1) in the second interval (in the vicinity of $E = 0.20$ V), and only state H(0) in the third interval including the monolayer formation at $E = 0.05$ V.

In this experiment, the alternating current was fixed, the same as the charge density amplitude Δq of the electrode which defined (in electrical units) the amount of hydrogen entering one of the states from the solution when the potential corresponded to the frequency-independent interval: $H^+ + e^- \to$ H(0), H(1), H(2). During transitions, that is as the filling increased, there was a sharp fall in repulsion created by a hydrogen atom along the surface. At the intervals of

transitions, the solid platinum surface tension anomalously increased with increasing surface concentration of hydrogen (an inverse relation is considered to be normal). The hydrogen contribution to the surface tension can be represented in electrical units as a function $\Gamma(E)$ with stepwise falls in the vicinity of transition potentials $E_{21} = 0.25$ and $E_{10} = 0.12$ V. In this case ($q < 0$, $\partial\Gamma/\partial E < 0$) one obtains

$$\frac{\partial\gamma}{\partial q} \approx -\Gamma - q\frac{\partial E}{\partial q}\frac{\partial\Gamma}{\partial E}\,. \tag{8.1}$$

The term $\partial\Gamma/\partial E$ is small at a distance from the transition potentials, and

$$\frac{\partial\gamma}{\partial q} \approx -\Gamma \tag{8.2}$$

regardless of the frequency which does not influence the contribution of a hydrogen atom to γ. In the vicinity of the transition potentials, the quantity $\partial\Gamma/\partial E$ becomes large, and $\partial E/\partial q$ grows with frequency due to a decrease in the capacitance $\partial q/\partial E$ (fewer ions could discharge at a fixed potential amplitude ΔE). Therefore, at high frequencies we have

$$\frac{\partial\gamma}{\partial q} \approx -q\,\frac{\partial E}{\partial q}\,\frac{\partial\Gamma}{\partial E}\,, \tag{8.3}$$

which is manifested as extrema, the heights of which increase with increasing frequency (minima of $\partial\gamma/\partial q$ or maxima of $|\partial\gamma/\partial q|$). The electrode acquires a negative charge when hydrogen ions undergo discharge to the adsorbed state. The multiplier q (with the opposite sign) gives the amount of hydrogen localized on the surface at the transition potential. The adsorption interval lies between $E = 0.5$ V (in the absence of hydrogen) and $E = 0.05$ V (monolayer).

When two steps of a change in the electron cloud dimensions are roughly identical, variations of contributions must also be equal: $(\partial\Gamma/\partial E)_{21} \approx (\partial\Gamma/\partial E)_{10}$, where the indices correspond to the potentials E_{21} and E_{10} of the minima. The ratio of the depths of these minima is equal to

$$\frac{(\partial\gamma/\partial q)_{10}}{(\partial\gamma/\partial q)_{21}} = \frac{q_{10}(\partial q/\partial E)_{21}}{q_{21}(\partial q/\partial E)_{10}}\,. \tag{8.4}$$

It follows from the data on the charging current j (see Fig. 11a) that $q_{10}/q_{21} = 2.8$ (from the area under the current curve) and $(\partial q/\partial E)_{21}/(\partial q/\partial E)_{10} = 0.66$ (the ratio of maximum capacitances which remains approximately unaltered with increasing frequency). Hence, $(\partial\gamma/\partial q)_{10}/(\partial\gamma/\partial q)_{21} = 1.9$, whereas in the hindered adsorption experiment (see Fig. 11b) this ratio was 1.7.

When the discharge of hydrogen ions is arrested almost completely (see Fig. 11b, frequency + cooling), the extrema T_{21} and T_{10} are separated by the segment H(1) which may all but vanish when very few new atoms reach the surface. This observation provides additional evidence that the transitions do not overlap and are completed (one independently of another) by all hydrogen atoms located at the surface.

Both transitions are apparent as the elongation of the binding electron cloud normal to the metal surface which, in the case of hydrogen, is almost equivalent to a lengthening of the distance between the centers of hydrogen and platinum atoms. In a monolayer, all hydrogen atoms keep identical positions at the metal surface.

The formation of a monolayer on coating the metal by external atoms is well apparent on the oscillograms (see, for example, a steep rise originating at the point shown by the arrow and marked with symbol $\mathcal{M}$ in Figs 11 and 12). Hydrogen adsorption continues with much greater repulsion during a subsequent cathodic shift of the potential when it involves atoms of the underlying (deeper) layer of the metal.

Surface tension data obtained before the monolayer is filled, in conjunction with Eqn (3.2), indicate that in the course of elastic surface extension, the number of hydrogen atoms per unit area in each state (frequency-independent sections) increases ($\partial q/\partial\Omega < 0$): that is the Pt–H bond strengthens as the distance between individual platinum atoms increases. Such a situation is feasible if a hydrogen atom is directly bound to a single Pt atom and immediately overlies it.

A change in the number of wave function nodes. The property of all the adsorbed atoms to remain in the same state after partial filling of the surface and collectively escape this state indicate that they are interconnected via the d-zone of the metal surface. Because the d-functions only slightly overlap, they largely keep the same shape as in isolated metallic atoms, provided there is no strong perturbation from the outside.

A remarkable finding is the coincidence between the number of adsorption transitions and that of the finite nodes of the radial component of the metal wave d-function. Indeed, there is one transition and one node of the 4d-function on rhodium, and two transitions and two nodes of the 5d-function on platinum and iridium. In conjunction with experimental data, this suggests the following mechanism of hydrogen adsorption. The initial state is due to the overlap between the 1s-function of a hydrogen atom and the d-function of a surface metal atom having one (Rh) or two (Pt, Ir) nodes. The nodes of the binding wave function of the metal consecutively disappear as the filling and potential jump increase. As a result, it takes the form

$$\begin{aligned} &\mathrm{Pt,Ir}\colon 5\mathrm{d}\{\mathrm{H}(2)\} \to 5\mathrm{f}\{\mathrm{H}(1)\} \to 5\mathrm{g}\{\mathrm{H}(0)\}\,,\\ &\mathrm{Rh}\colon 4\mathrm{d}\{\mathrm{H}(1)\} \to 4\mathrm{f}\{\mathrm{H}(0)\}\,, \end{aligned} \tag{8.5}$$

where the number of finite radial nodes corresponding to a definite state of the adsorbed hydrogen is given in parentheses (Fig. 14). The radial node at infinity inherent in all wave functions remains unaltered. A state without internal nodes constitutes a natural limit since further evolution of the wave function retaining its symmetry would require an enhancement of the principal quantum number.

The above shapes of the wave function are not typical of the ground state of an isolated metal atom. They arise here as a result of the double-layer field effect on the binding electron pair which includes the hydrogen s-electron. Results of the experiment (see Fig. 11b) in which transitions occurred without a change in the total number of adsorbed atoms confirm the key role of the double-layer field. Discrete elongation of the bond with field strengthening would have taken place even if only one hydrogen atom had been adsorbed at the metal surface. The relative contribution of the ionic atmosphere and Pt–H dipoles to the double-layer field depends on the degree of a surface filling. The contribution of dipoles prevails when hydrogen is adsorbed from a gaseous medium.

The phenomenon under consideration differs from term splitting in a ligand field during metal complex formation.

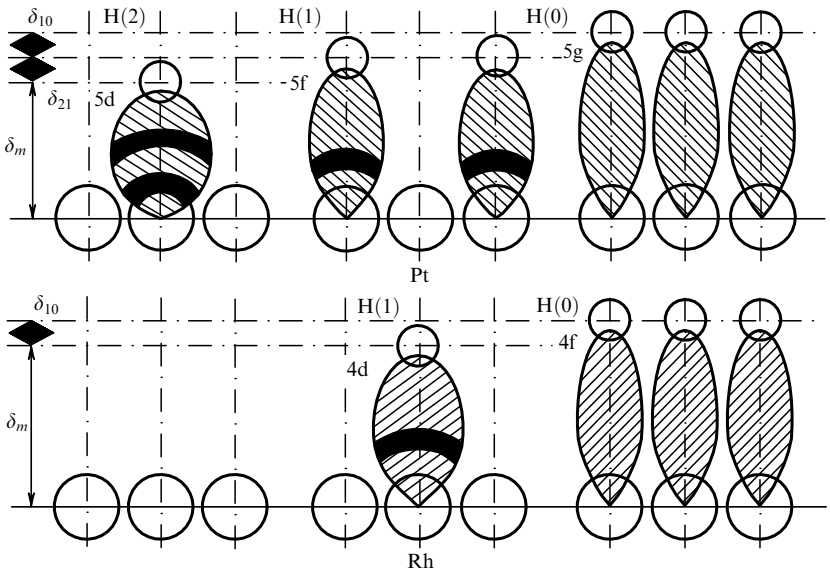

Figure 14. Schematic representation of the consecutive exclusion of the wave function nodes of surface metal atoms with increasing number of adsorbed hydrogen atoms and a double-layer field. Two elongation steps of the metal – hydrogen bond $\delta_{21} \approx \delta_{10} \approx 0.2$ Å on platinum and one step δ_{10} on rhodium; δ_m — initial bond lengths. The diagram shows the evolution of central petals of the wave functions (for a zero magnetic quantum number) on the assumption of smallness of the overlap between these functions in the adjoining metal atoms.

The ligand field acts on a metal ion and removes the degeneracy of the levels, but it is not an external factor able to discretely modify the state of the resulting complex compound. Electron transitions between term levels are feasible under effect of an additional factor, for instance, radiation. The fields of interacting particles play a similar role during the formation of cluster ions [39].

In the course of hydrogen adsorption, metal ions are screened from the double-layer field while a discrete change in the state of adsorbed atoms represents a response to the field alteration as an external factor which confers an additional energy on the surface metal – hydrogen compound (Pt – H, Rh – H). In the potential interval between transitions, the energy of the surface compound grows continuously with increasing field. The intervals between discrete energy levels found from the base width of the observed peaks are close to 0.1 eV. The corresponding lines in the optical spectrum of a given metal lie in the far infrared region (wave number of the order of 1000 cm^{-1}) and seem to be indiscernible among hundreds of other lines.

The spatial deformation of wave functions in the d – f – g sequence can be qualitatively evaluated from their angular constituent $Y_{l0}(\theta)$ (for zero magnetic quantum number) known for the hydrogen atom [40]. As the orbital quantum number $l = 2, 3, 4$ grows, its length $Y_{l0}(0)$ along axis $\theta = 0$ also increases while the angle $2\theta_{l0}$ formed by the main petal at the origin of the polar coordinate system (in the center of the atom) decreases: d — $Y_{20}(0) = 0.631$, $\theta_{20} = 55°$; f — $Y_{30}(0) = 0.746$, $\theta_{30} = 39°$; g — $Y_{40} = 0.846$, $\theta_{40} = 30°$. For a certain form of radial constituent, this row of values is equivalent to the elongation of the binding orbital and the decrease of its transverse dimension with growing orbital momentum.

In platinum and rhodium with more than five d-electrons, the field generated by an atomic core may be assumed to be spherically symmetric; this makes it possible to use the hydrogen-like shape of the angular constituent of the wave d-function. The obvious similarity between the above oscillograms for two metals confirms the important role of the shape of the angular constituent in the phenomenon being considered.

The radial constituent is subject only to qualitative assessment to illustrate the physical sense of the observed wave-function deformation. The evaluation is based on the concept of the screening charge of internal electrons σ_{nl} and the quantum defect δ_{nl} [41]. In a state with the principal quantum number n, the mean distance between an electron and the nucleus with charge Z can be represented as

$$r_{nl} = \frac{a_1\left[3(n-\delta_{nl})^2 - l(l+1)\right]}{2(Z-\sigma_{nl})}\,, \tag{8.6}$$

where a_1 is the Bohr radius. For hydrogen, $\delta_{nl} = \sigma_{nl} = 0$, $Z = 1$ which accounts for a decrease of r_{nl} at $n = \text{const}$ with growing l, i.e. in the s – p – d – f – g series. The situation changes in the case of heavier atoms. A rise in the orbital momentum decreases the probability of finding an electron in the atomic core region and thus leads to a decrease in the quantum defect δ_{nl} and enhancement of screening charge σ_{nl}. For $n = \text{const}$, both these factors contribute to the rise of r_{nl} with increasing l, their effect exceeding that of the term $l(l+1)$.

The two varieties of wave function deformity have been observed in experiment. The elongation of the adsorption bond in two steps of 0.2 Å each leads to the enlargement of the electrode volume and produces two negative peaks on oscillograms of $\partial\delta/\partial q$ (see Fig. 13). A decrease in the transverse dimension of the binding orbitals is responsible for the impaired mutual repulsion of electron pairs in adjacent orbitals and the enhanced surface tension of a solid metal. These changes are apparent as two negative peaks on oscillograms of $\partial\gamma/\partial q$ (see Fig. 11a,b and Fig. 12 which gives $|\partial\gamma/\partial q|$). The coincidence of signs in $\partial\delta/\partial q < 0$ and $\partial\gamma/\partial q < 0$, seen during each transition, implies that

$$\{\Delta\delta > 0\} \to \{\Delta\gamma > 0\}\,. \tag{8.7}$$

Hence, the elongation of the binding electron cloud is paralleled by its transverse compression (see Fig. 14).

Consecutive deformations of the wave function being of similar magnitude, this accounts for the roughly identical contribution of H(2)–H(1) and H(1)–H(0) transitions to a decrease of surface tension and an increase of volume (the elongation of bond, $\delta_{21} \approx \delta_{10} \approx 0.2$ Å, in each transition in platinum). The relative elongation of the d-orbital can be approximately estimated by taking advantage of the known atomic radius of platinum, $r_0 = 1.387$ Å. Then, $\delta_{21}/r_{52} \approx \delta_{21}/r_0 \approx 0.144$ (from experiment). The corresponding deformation of the angular component $[Y_{30}(0) - Y_{20}(0)]/Y_{20}(0) = 0.182$. At the next elongation step, $[Y_{40}(0) - Y_{30}(0)]/Y_{30}(0) = 0.134$.

Given the proximity of elongation steps for an individual Pt–H bond, the heights of consecutive peaks on the oscillograms are largely dependent on the number of hydrogen atoms present on the surface at the potential of the corresponding peak. A greater size of the second peak compared with that of the first one gives further evidence in support of the proposed mechanism of adsorption. Experimental data including direct measurements of deformation by independent methods suggest a discrete change of the wave function geometry; there is no argument that contradicts this finding.

The above analogy with the theatre as a model of two kinds of seats can be used here to illustrate the collective character of adsorption-related transitions and to compare the efficiency of different experimental tools. The method of current allows the discharge of hydrogen ions, i.e. their ascent from the solution to the surface, to be detected. In a figurative sense, it functions as a doorman standing at the entrance to the theatre and counting all those who pass on their way in. He can have no idea of what takes place inside if there are no (or few) visitors. The method of surface tension evaluates the state of the surface at any frequency. It is an usher in the auditorium who sees that only the parterre, looking like a level plot, is accessible to the audience. Those who arrive first lie on the floor. After the floor is totally occupied, all the people take seats. As the auditorium becomes overcrowded, they all have to stand up to make room to newcomers who all are standing. In the end, all those present are on their feet in the parterre, and it is impossible to know who came earlier and who was the last to arrive.

It is the very last spectator entering the auditorium and finding no vacant place for himself who makes all the rest stand up. The current technique identifies each new person coming in but fails to distinguish him or her from the previous one in terms of importance for the final situation. In the context of the tension method (and for all those who are already inside the theatre), the passage of a certain newcomer is paramount and has far more serious implications than those of his (her) predecessor.

The above analogy considerably simplifies the real conditions under which both the overcrowding and the mode of its management depend on a concrete situation. Transverse narrowing of each atomic orbital is not so much the result of tightness as that of transition to an excited state upon absorption of a certain amount of the growing double-layer energy. In the meantime, a cram exists. When it is lessened, the reduction is apparent as a stepwise rise in the surface tension the derivative of which has the form of an isolated peak.

Peak disconnection eventually leads to a homogeneous monolayer. The surface tension method and electrocapillary expansion technique are mutually complementary in that they reveal a change of the wave function in two projections, along and normal to the metal surface. Taken together, they provide an abstract stereographic picture of this quantum object divided by nodes.

9. Irreversible coating with memory

Discrete phenomena observed during hydrogen adsorption also pertain to a more general problem of electron configuration of heavy atoms in their chemical compounds. Effects analogous to those described in previous sections may be equally important in the adsorption of other substances.

Hydrogen adsorption makes these effects accessible for direct observation by virtue of the readily apparent dynamics of consecutive transformations. In more complicated cases, the dynamics may not be observed because the number of nodes of the wave function changes concurrently with the formation of a compound, either in the homogeneous phase or at the interface. The surface is somewhat superior to the volume of the condensed phase in terms of wave function deformation due to the possibility of free motion along the normal. Symptoms of a two-step change in the bond length have been recorded during the adsorption of a fluorine atom on mercury from an aqueous NaF solution, namely, two capacitance and $\partial\gamma/\partial q$ waves till the monolayer is formed (see Fig. 4). This process may be considered as associated with the transition 6p → 6d → 6f in the surface Hg–F compound.

Another example of a probable exclusion of wave function nodes is oxygen adsorption on metals. Surface tension oscillograms of platinum and rhodium have similarly shaped oxidized portions (Fig. 15a, b). Oxygen adsorption is responsible for two characteristic features, R_0 and R_a, on platinum and one, R_0, on rhodium. This is like the difference in the hydrogen adsorption region described earlier (two transitions T_{21} and T_{10} in platinum and one, T_{10}, in rhodium). Owing to the relatively large atomic size of oxygen, its adsorption on metals is a more complicated process than that of hydrogen adsorption. Also, it shows the greater dependence on the external conditions. In this context, hydrogen is more suitable for probing a metal surface, but comparison with oxygen provides additional information.

Hydrogen adsorption is totally reversible. Its region on oscillograms of platinum and rhodium is readily distinguishable thanks to the coincidence of the forward and backward motion of the beam on the dependence $|\partial\gamma/\partial q| - E$ (see Fig. 15). Oxygen adsorption is reversible only up to a certain potential E_R (0.8 V for platinum, and 0.7 V for rhodium) corresponding to an extremum of R_0. It is unilateral and reached only with increasing E. Under these conditions, the charge increment $\Delta Q > 0$ ($\Delta q > 0$) of the electrode (Pt, Rh) corresponds to the inequalities $\Delta\gamma < 0$ (enhanced repulsion) and $\Delta V < 0$ (decreased volume of the system due to the interface thinning, see Fig. 13).

To summarize, experimental studies have demonstrated that the oxygen atom is reversibly wedged between surface atoms of the metal as the positive charge at the metal surface increases. As soon as the oxygen atom reaches the bottle neck, i.e. under maximum repulsion, it penetrates deeper into the surface layer of the metal and thus avoids the influence of the double-layer field. With further progress of oxidation, the dependence on the potential becomes weaker and irreversible until $E > E_R$.

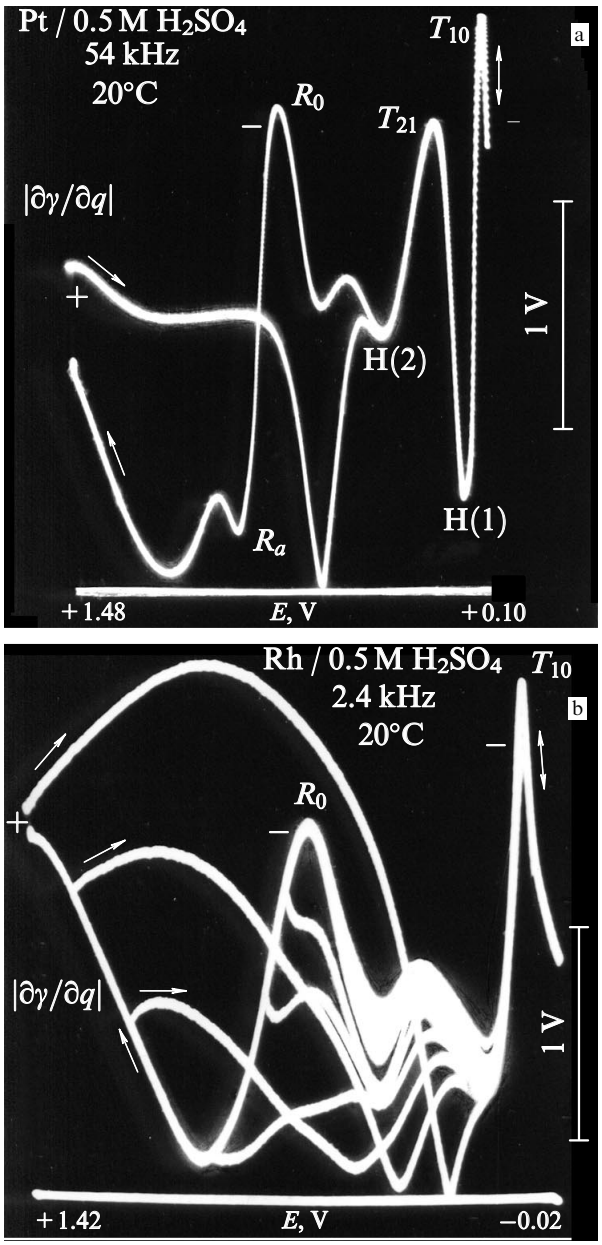

Figure 15. Surface tension oscillograms of platinum (a) and rhodium (b) illustrating the memory effect of an oxidized surface; surface orientation (100). Noteworthy are similarity of the shape of reversible peaks T_{10} and proximity of their positions on the potential axis for either metal.

No matter how deep is the metal surface affected by oxidation at a high anode potential, the return to the cathode region, $E < E_R$, reproduces the initial state of the surface. Curves which are markedly different in the anode region in terms of the degree of oxidation practically coincide after the return to more negative potentials (see Fig. 15a,b). The surface possesses the property of memory. It is nontrivial because progressive oxidation leads to a change in the metal structure beneath the monolayer.

Cathodic reduction of the oxide layer creates conditions for surface recrystallization. Coincidence of consecutive oscillograms in the cathode region indicates that the recrystallization is complete. Oscillograms obtained with rolled and annealed platinum and rhodium plates coincide beginning from the very first scan in the cathodic direction; this suggests regular features of the surface which are preserved after anode treatment.

These findings indicate that the degree of surface state reversibility depends on the field of the double layer. The irreversible anodic state of platinum and rhodium is maintained by the field ($E > E_R$) and decays after its removal. Under certain conditions, the irreversibility in relation to the potential may result from the screening of the adsorbed atom by electrons of the metal.

10. Membranes and their precursors

The activity of living organisms is to a large extent dependent on a flow of electric current through cell membranes some 50 – 100 Å thick. This process underlies metabolism and the propagation of a sequence of coded impulses passing along a nerve fibre. In a paper published in 1800, Volta compared his battery with the electric organ of fish. The electric eel *Electrophorus electricus* is known to generate current pulses of 1 A at voltages as large as 1000 V. Its electric organ of more than a meter in length is composed of thousands of controllable flattened cell elements separated by plasma membranes and arranged in series. Such a complicated structure is a product of specialized evolution which must have started from a low-voltage-producing progenitor. It is believed that initially the electric organ was not intended to stun or kill prey; rather, it might have been used for sensing purposes.

Certain fish species have been reported to show high susceptibility to an electric field in water (at a threshold value of 1 μV cm^{-1}) [42]. Equally with electroreceptors on their heads, these species have specialized organs emitting electrical signals which serve for sensory location and communication. The characteristics of the signal received (magnitude, form, and delay) are encoded by receptor cells as a sequence of equally strong potential pulses.

The potential difference across a membrane (50 – 100 mV) is created in animal cells by the transport of sodium ions from the inner membrane surface to the outer one. The process involves two components which Volta regarded as indispensable: "la fanno un tempo stesso da motori e da condensatori" (in the given case, this occurs owing to *motors* and *capacitors*) (from a letter written in August 1796). The motor is the 'sodium pump', and the capacitor is formed by two solutions separated by a membrane.

The membrane is a two-layer structure called a bilayer and composed of lipid molecules whose phosphate groups face out on each cell surface. Enzyme proteins embedded in the phospholipid matrix cannot function normally unless there is a certain potential change due to the presence of excess ions in the solutions. Moreover, 20% of the phosphate groups at either membrane surface carry a negative charge which coordinates enzyme location and affects the concentration of excessive ions. The distance between localized charges at the membrane surface is close to 20 Å. Therefore, three potential changes are actually essential: one inside the membrane and two others in the diffuse double layers near their surfaces [43].

Spiral channels in the lipid double layer can serve for the free flight of protons whose energy is liberated in the form of ultraviolet radiation upon subsequent collisions [44].

In this situation, as in the case of discharge on a metal (see Sections 4 and 5), the energy acquired by a proton in the membrane field is limited by the discreteness of excess charges on either side of the membrane. The membrane thickness δ_m is

one order of magnitude greater than the thickness of the double layer at the metal–solution boundary. However, it remains as usual less than the mean distance λ between excess ions in the ionic atmosphere. In the case of regular hexagonal arrangement of the ions, it is estimated to be $\lambda = 145$ Å at $\delta_m = 50$ Å, $\varepsilon_s = 5$ (mean values for the inner and outer sides), $C_i = 1\ \mu\text{F cm}^{-2}$, and $\eta = 0.1$ V, typical for normal membrane parameters. Hence, and from the data reported in Section 5, $\theta = \lambda/\delta_m = 2.9$, $\eta_r/\eta = 0.44$, and $\chi_0 = \eta_r/2\eta = 0.22$ to ensure the translocation of an elementary charge across the membrane, rapid enough if compared with the relaxation time of the ionic atmosphere.

The effect of quantum insulation in the proton transition is small and $\chi \approx \chi_0$. In this case, $\alpha = \vartheta + \chi \approx 0.50 + 0.22 = 0.72$. In other words, the proton acquires an energy of $\alpha e\eta \approx 0.072$ eV on its free path in the membrane field.

The time of flight of a proton is $\tau_p = 2.7 \times 10^{-12}$ s or an order of magnitude less than the time needed to fill the vacancy, $\tau_v = \lambda(\rho_m + \rho_n)C_i$, where ρ_m and ρ_n are the resistivities of intra- and extracellular solutions, respectively, each in excess of 20 Ω cm (for an exact calculation, membrane surface conductivity needs to be taken into consideration).

The Boltzmann distribution function and the Gouy theory are the major tools employed to calculate parameters of biological bilayers. It follows from the results presented in Section 7 that this approach tends to underestimate the ion concentration near a membrane surface, the error increasing with dilution strength. This finding has especially important implications for electrokinetic experiments in which the surface charge of the membrane is evaluated. When ion concentrations near the membrane surface are measured in 10^{-3} M solutions, the error may be as large as 100%. The more accurate calculation is possible using the equations presented in Section 7.

Specialized electric circuits in the plasma membrane coexist with intracellular ones. There are numerous anaerobic bacteria producing hydrogen in the reactions catalyzed by the enzyme hydrogenase. Results of X-ray structural analysis [45] indicate that the enzyme contains, besides protein moiety, six clusters of ferrous sulfide, FeS, arranged in a chain of four serially connected groups. The 50-Å long chain includes 20 iron atoms. One of its terminal sequences contains a H_2O molecule and five CO molecules as ligands. This end is involved in the reaction $H^+ + e^- \rightarrow H$, $2H \rightarrow H_2$. Protons from the surrounding solution (hydrogen ions) enter through a protein channel. The opposite terminus is periodically bound to the enzyme ferredoxin which brings electrons from glucose. The principle of action of this bacterial apparatus is similar to that of Volta's element with one metal and two solutions. The frequency of repeat cycles is $10^6\ \text{s}^{-1}$, which is equivalent to a current density of the order of 1 A cm^{-2}. One effective technique for the study of catalytic properties of enzymes is their adsorption on electrodes [46].

Hydrogen production was the primary activity of primitive organisms at the early stages of life. The technology of this process was improving over 2 billion years, since the formation of the Earth till the Late Archean 2.5 billion years ago. The Earth's atmosphere was initially a mixture of CO_2, N_2, and H_2O with traces of hydrogen [47]. The oxygen content reached 1% of the present-day level only in the Late Proterozoic Era, i.e. 1 billion years ago. That was the time when the simplest multicellular organisms came into existence.

Hydrogen (in conjunction with specific enzymes) always served as a strong reducing agent, in the first place to convert CO_2 into a carbon-containing compound (CH_2O) and also for nitrogen fixation. As the primitive organisms evolved into more highly organized ones, the process of hydrogen consumption was paralleled by the development of different modes of its production. The most effective turned out to be decomposition of water into hydrogen and oxygen using solar radiation energy. The first photosynthetic cells, blue–green algae, are thought to have appeared 3 billion years ago. They were preceded by sulfur bacteria which took advantage of gaseous H_2S, a product of volcanic activity, as the source of hydrogen.

Although hydrogen atoms in H_2S are bound much more weakly than in H_2O (4.8 and 68.3 kcal mol^{-1}, respectively), specific enzymes are needed to withdraw them from either compound. Under the Archean conditions, such enzymes came into being with a time constant of approximately 1 million years. It is therefore natural to assume that another source of hydrogen, more readily accessible for its direct consumption than the volcanic gas, had been available before sulfur bacteria began using H_2S.

The Earth's crust is thought to have formed in the Early Archean and its predominant part has been initially covered by the ocean. Meteoritic falls, earthquakes, and eruptions of magma were very common. Archean rocks are known to contain iron, copper, lead, and zinc sulfide deposits along with inclusions of gold, silver, nickel, and some other metals. Many sulfides are characterized by high electric conduction of a metallic (CuS_2) or impurity (FeS_2) kind. Massifs of different electron conductors were in contact with one another at the ocean floor where they were washed with a 0.1 M NaCl solution and incidentally renewed. In other words, the natural conditions of that time closely resembled the situation in Volta's experiments and could therefore bring about similar results.

Pyrite FeS_2 (large golden crystals showing hard brilliance like that of metals) and pyrrhotite FeS (dark-brown crystals) are most common natural sulfides. Their association in an aqueous medium (0.1 M NaCl) may produce an electromotive force of 0.3 V similar to that generated in the presence of iron and silver (0.4 V). In a series of voltages, they keep the following positions with respect to iron: Fe–FeS–FeS_2. At low current densities, pyrite keeps nearly the same place as silver. In a FeS_2/FeS pair, part of the hydrogen released on pyrite undergoes absorption and saturates the surface layer of the mineral while pyrrhotite gives rise to dissolved iron: $2FeS \rightarrow 2Fe^{2+} + S_2 + 4e^-$.

In this situation the current density is small (from 0.1 to 1 mA cm^{-2} depending on the convection of the solution) but sufficient to ensure that all hydrogen necessary for a 1-μm thick cell monolayer at the pyrite surface is released during 1 hour provided that the cells are either permeable or fail to occupy the entire mineral surface. Inclusions of metals occurring in veins or disseminated throughout other minerals participated in the formation of more powerful sources of electric current. In large rock massifs, such as cliffs composed of different electroconductive minerals, electric current could pass through a water column far from the source and thus promoted hydrogen accumulation either in pores or in an absorbed form.

Earthquakes caused rapid redistribution of water in the primeval ocean. Its stony floor was the safest place for the development of life. At the initial stage of the formation of

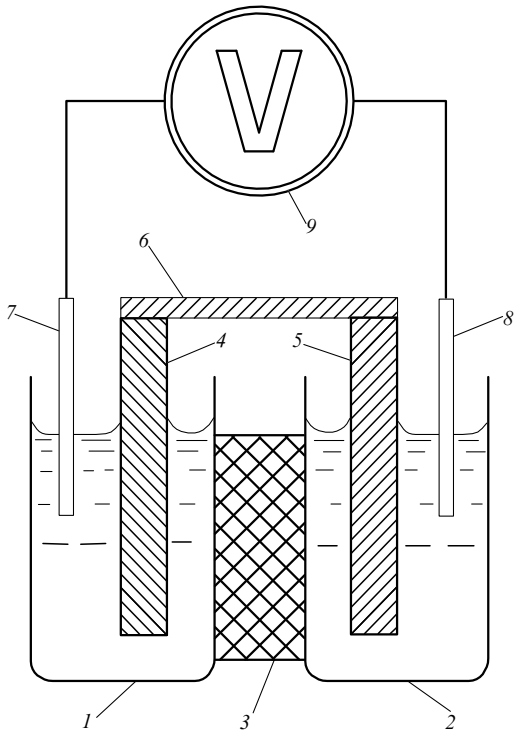

Figure 16. The mechanism of formation of a transmembrane potential in a system with two different conductors in contact with each other: *1*, *2* — solution-containing vessels; *3* — partition functioning as a membrane; *4*, *5* — different electron conductors (FeS_2 and FeS); 6 — shunt (any of the two conductors); *7*, *8* — identical probes; *9* — voltmeter measuring the potential jump across the partition.

self-contained cells, membranes might serve as envelopes fastened on the perimeter to an electroconductive mineral. Given a sufficiently large number of neighboring cells responsible for the impaired shunting effect, each envelope experienced the potential difference (see Fig. 16), and was able to modulate it by virtue of its own resistance and use it for the transport of ions and associated molecules.

In this model, the coating of a major part of the mineral surface provided an important advantage in terms of utilization of the electric current. This, in turn, contributed to the ability of the membrane to grow along the surface and divide (for better mechanical strength) into separate portions. Polymer chains showing the maximum growth rate predominated and were gradually elaborated, thus promoting the restoration of a disturbed coating or giving rise to a new one in those places to which they were brought by water...

[*Notes added in proof*: The negative polarity of the cell interior is probably inherited from that time when membranes were conceived on the sulfide cathode as the source of hydrogen in the primeval ocean where free oxygen was absent and hydrogen ions were delivered by carbon acid. Within pH range from 3 to 9, the cathodic dissolution of iron sulfides takes a relatively small part of the current. Absorption of atomic hydrogen shifts the sulfide potential E_S to the negative direction almost linearly with growth of the hydrogen concentration c_H in the interval $0 < E_S < 0.7$ V relative to the iron electrode.

In the solution 0.1 M KCl + 0.5 M $KHC_8H_4O_4$ in argon atmosphere, the absorption capacities $\Delta c_H/\Delta E_S$ measured at 20°C are 4×10^{-4} and 2×10^{-3} mol dm^{-3} V^{-1} for pyrite and hexagonal pyrrhotite, correspondingly. The diffusion coefficient of H in pyrite is by an order of magnitude greater than in pyrrhotite for which the value 4×10^{-6} cm^2 s^{-1} was obtained.

The iron – nickel meteorites without oxide covering can serve as anodes with respect to monolithic pyrite or pyrrhotite. In the chloride solution, the potential of the meteoritic alloy with 5% Ni is only by 20 mV more positive than that of iron. A porous pyrrhotite containing a mixture of small grains with excess and deficiency of iron ($Fe_{1+x}S$, $Fe_{1-x}S$) makes an effective anode in couple with the monolithic sulfides. Wetting it by aqueous solution makes it close to iron in the potential series.

More detailed description of experiments concerning electrolytic hydrogen in sulfides is supposed to be published in the journal *Protection of Metals* (2001)].

The discovery of electric current was made on the borderline of physics and biology. Modern molecular biology has accumulated numerous experimental data on the structure of proteins and nucleic acids. These substances are considered to be a sum of atoms, which gives hope that 'the molecular logic of life' will be explained based on known laws.

The most difficult thing is to find out the physical conditions in which a combination of abiogenic elements produces a living organism with an abstract content. Within a certain limit, this content is invariant, i.e. independent of the alphabet used, and therefore primary which is crucial for the maintenance of life.

The progress of biological evolution over 4 billion years is apparent from the size of genomes of existing species [48, 49]. These vary from 5×10^3 nucleotides in the single-stranded bacteriophage DNA to 3×10^9 nucleotide pairs in the double-stranded DNAs of the frog and man, and even 5×10^9 pairs in corn. Evidently, the final rate of evolution achieved in the frog, man, and corn is unrelated to natural selection; hence, it must have been governed by general physical laws.

Some repercussions of these subtle effects can be found at interfaces between two media. Apart from purely scientific interest, this problem has important practical implications. The investigation of biological systems opens prospects for the development of ecologically friendly technologies. Enzymatic catalysis provides a tool for increasing reaction rates by a few orders of magnitude at a reduced energy expense. The action of hydrogenase is one of many examples.

The working mechanism of such systems is difficult to realize, largely because it is underlain with so far unknown physical principles. The protein structure is known to be maintained by virtue of a spatial charge region of which the simplest and most characteristic specimen is the electrical double layer. Results of the above stepwise adsorption experiments indicate that the total electric field is an important collective factor facilitating the occupation of vacant orbitals in the system and thus influencing its conformation.

Interface properties are related to charge discreteness and spatial localization of energy. Nature knows the secrets of these phenomena and exploits them to the utmost completeness. The use of all pertinent physical laws and accumulation of information about them constitute the main principle of the logic of life which has been operating for several hundred million years. Should the situation with the interrelation between physics and biology, like that which resulted in the discovery of the electric current, ever arise again, it may bring about equally surprising and useful findings.

11. Conclusions

Known physical phenomena may be considered as elements of a certain space with an established basis and plenty of room for the construction of novel theoretical concepts. At the end of the 19th century, the ideal (i.e. complete basis) seemed to be achieved. Today, however, broadening the basis is as topical as it was in the 18th century and also requires independent experimental approaches.

After two hundred years, Volta's discovery remains a landmark event on this route. The breakthrough of the boundaries of the known basis and the enhancement of the spatial dimension of natural phenomena are so perfectly evident that they acquire literal meaning. Current intensity and its dimension were lacking from the initial basis. The combination of metals with a solution created conditions for the examination of the interface between two media. Decomposition of a substance by electric current at the interface provided the basis for a far-reaching concept of the involvement of electric forces in the structure of matter.

The passage of electric current through the interface always posed two sorts of problems, one concerning the mechanism of charge transfer, the other the state of the interface. Analysis of these problems in the present paper took into account recently discovered general phenomena: quantum discharge insulation and spontaneous condensation of the ionic atmosphere.

The quantum delay of energy transfer along the double layer accessible to observation provides independent information about the evaluation of the space–time phase-boundary structure and the identification of the particle species carrying the current. The mean force of ion attraction is used as an alternative tool to address the theory of double layer allowing us to take charge discreteness in the ionic atmosphere into consideration and find the critical potential limiting the capacitance minimum width. Concentrated forces in the spatial charge region are also essential for the maintenance of the conformation of protein molecules.

Surface phenomena being varied and complicated, their observation still encounters difficulty for the lack of adequate experimental tools. The above results were obtained due to the advent of new methods and instruments which may just as well be applied in different fields. Methods having no analogues include the detection of alternating surface tension of solids. These were used, for example, to observe stepwise deformation of the wave function of a metal atom associated with adsorbed hydrogen.

The discrete growth of the orbital momentum is accompanied by the elongation of the wave function in the direction of the bond and the reduction of its transverse dimension which collectively lead to an increase in the number of particles adsorbed on the metal. Further studies of the phenomenon of interest directly observable in two projections may bring new independent data concerning the nature of bonding both at the surface and in the bulk of the substance. Also, they may highlight the effects of orbital momentum on the geometry of wave functions of heavy atoms.

Further progress in the physics of surface phenomena will offer prospects for research and development of novel technologies including the search for surface structures to be used in enzymatic catalysis.

The author is grateful to B M Smirnov for an interesting discussion of the material of this paper and helpful comments.

References

1. Volta A *Le Opere di Alessandro Volta* Vols 1 – 7 (Milano: U. Hoepli, 1918 – 1929)
2. Maxwell J C *A Treatise on Electricity and Magnetism* 3rd ed. (Oxford: Clarendon, 1892) [Translated into Russian (Moscow: Nauka, 1989)]
3. *James Clerk Maxwell Commemorative Booklet* (Edinburgh: J.C.M. Foundation, 1999)
4. Galvani L *De Viribus Electricitatis in Motu Musculari Commentarius* (Prague: J.G. Calve, 1973; Norwood, Conn.: Burndy Library, 1953)
5. Polvani G *Alessandro Volta* (Pisa: Domus Galileana, 1942)
6. Faraday M *Experimental Researches in Electricity* Vol. 2 (London: B Quaritch, 1844)
7. Helmholtz H *Pogg. Ann. Phys.* **89** 228 (1853)
8. Lippmann G *Ann. Chim. Phys.* **5** 494 (1875)
9. Heyrovský J, Kúta J *Základy Polarografie* (Praha: Nakladatelstvi Československé Akademie Věd, 1962) [Translated into English: *Principles of Polarography* (Prague: Publ. House of Czechoslovak Acad. of Sciences; New York: Academic Press, 1966)] [Translated into Russian: *Osnovy Polyarografii* (Moscow: Mir, 1965)]
10. Gokhshteĭn A Ya, Gokhsteĭn Ya P *Zh. Fiz. Khim.* **36** 651 (1962)
11. Gouy G *C. R. Acad. Sci.* **146** 612 (1908)
12. Frumkin A, Gorodetzkaya A *Z. Phys. Chem.* **136** 451 (1928)
13. Frumkin A N *Potentsialy Nulevogo Zaryada* (Zero-Charge Potentials) (Moscow: Nauka, 1979)
14. Gokhshteĭn A Ya *Poverkhnostnoe Natyazhenie Tverdykh Tel i Adsorbtsiya* (Surface Tension of Solids and Adsorption) (Moscow: Nauka, 1976)
15. Tafel J *Z. Phys. Chem.* **50** 641 (1905)
16. Bockris J O'M, Khan S U M *Quantum Electrochemistry* (New York: Plenum Press, 1977)
17. Vetter K J *Elektrochemische Kinetik* (Berlin: Springer-Verlag, 1961) [Translated into English: *Electrochemical Kinetics; Theoretical and Experimental Aspects* (New York: Academic Press, 1967)]
18. Koryta J, Dvořák J, Kavan L *Principles of Electrochemistry* (Chichester: Wiley, 1993)
19. Kuznetsov A M *Charge Transfer in Chemical Reaction Kinetics* (Lausanne: Presses Polytechniques, 1997) p. 73
20. Gokhshteĭn A Ya *Pis'ma Zh. Eksp. Teor. Fiz.* **57** 69 (1993) [*JETP Lett.* **57** 74 (1993)]
21. Gokhshteĭn A Ya *Dokl. Ross. Akad. Nauk* **345** 57 (1995) [*Doklady Phys. Chem.* **345** 247 (1995)]
22. Gokhshteĭn A Ya *Dokl. Ross. Akad. Nauk* **350** 632 (1996) [*Doklady Phys. Chem.* **350** 263 (1996)]
23. Messiah A *Mechanique Quantique* (Paris: Dunod, 1959) [Translated into English: *Quantum Mechanics* (Amsterdam: North-Holland Publ. Co., 1961 – 1962)] [Translated into Russian (Moscow: Nauka, 1978)]
24. Feller W *An Introduction to Probability Theory and its Applications* 3rd ed. (New York: Wiley, 1967)
25. Einstein A *Ann. Phys.* (Leipzig) **17** 132 (1905)
26. Sass J K, Gerischer H, in *Photoemission and the Electronic Properties of Surfaces* (Eds B Feuerbacher, B Fitton, R F Willis) (London: Wiley, 1978) p. 469
27. Gokhshtein A Y *Spectroscopy Lett.* **32** 205 (1999)
28. Poisson S D *Memoires Acad. Sci.* **6** 441 (1827)
29. Gouy G *J. Phys. Radium* **9** 457 (1910)
30. Chapman D *Philos. Mag. Sixth Ser.* **25** 475 (1913)
31. Vorotyntsev M A, Kornyshev A A *Elektrostatika Sred s Prostranstvennoĭ Dispersieĭ* (Electrostatics of Media with Spatial Dispersion (Moscow: Nauka, 1993) pp. 89, 94, 103
32. Debye P, Hückel E *Phys. Z.* **24** 185 (1923)
33. Gokhshteĭn A Ya *Dokl. Ross. Akad. Nauk* **355** 58 (1997) [*Doklady Phys. Chem.* **355** 197 (1997)]
34. Grove W R *Philos. Mag. Third Ser.* **14** 127 (1839)
35. Breiter M W *J. Phys. Chem.* **68** 2250 (1964)
36. Zinola C F, Arvia A J *Electrochimica Acta* **41** 2267 (1996)
37. Gokhshteĭn A Ya *Dokl. Ross. Akad. Nauk* **349** 768 (1996) [*Doklady Phys. Chem.* **349** 203 (1996)]
38. Gokhshteĭn A Ya *Dokl. Ross. Akad. Nauk* **351** 59 (1996) [*Doklady Phys. Chem.* **351** 292 (1996)]

39. Smirnov B M *Kompleksnye Iony* (Complex Ions) (Moscow: Nauka, 1983)
40. Shpol'skiĭ É V *Atomnaya Fizika* (Atomic Physics) (Moscow: Nauka, 1984) [Translated into English (London: Iliffe Books, 1969)]
41. Smirnov B M *Fizika Atoma i Iona* (Physics of Atoms and Ions) (Moscow: Energoatomizdat, 1986)
42. Shepherd G *Neurobiology* (New York: Oxford Univ. Press, 1983) [Translated into Russian (Moscow: Mir, 1987)]
43. Gennis R B *Biomembranes: Molecular Structure and Function* (New York: Springer-Verlag, 1989) [Translated into Russian (Moscow: Mir, 1997)]
44. Kovarskiĭ V A *Usp. Fiz. Nauk* **169** 889 (1999) [*Phys. Usp.* **42** 797 (1999)]
45. Adams M W W, Stiefel E I *Science* **282** 1842 (1998)
46. Bogdanovskaya V A, Kuznetsova L N, Tarasevich M R *Elektrokhimiya* **35** 692 (1999)
47. Huber C, Wächtershäuser G *Science* **276** 245 (1997)
48. Vol'kenshteĭn M V *Obshchaya Biofizika* (General Biophysics) (Moscow: Nauka, 1989) [Translated into English (New York: Academic Press, 1983)]
49. Singer M, Berg P *Genes & Genomes* (Mill Valley, Calif.: Univ. Science Books, 1991) [Translated into Russian (Moscow: Mir, 1998)]